

**Republic of IRAQ**  
**Ministry of Higher Education & Scientific**  
**Research**  
**Al-Nahrain University /College of Science**  
**Department of Physics**



***X-ray Radiographic Study of Simulated Voids –  
Like Defects in Aluminum Casting and Welded  
Joints in Steel***

**A THESIS**

***Submitted to the***

***Physics Department, College of Science, Al-Nahrain University***

***In Partial Fulfillment for the Degree of Master of Science in Physics***

**By**

***FARQAD RASHEED SAEED AL-ZUBAIDY***

**B.Sc. Physics**

**Supervised By**

***Dr. Mazin F. Mahrok***


***Dr. Thamir A. Jumah***

**Shabaan 1431  
August 2010**

بِسْمِ اللَّهِ الرَّحْمَنِ الرَّحِيمِ

((وَأَنْزَلْنَا الْحَدِيدَ فِيهِ بَأْسٌ شَدِيدٌ وَمَنْفَعٌ لِلنَّاسِ))

صدق الله العظيم

قران كريم  
سورة الحديد  
اية (25) 

قال رسول الله (صلى الله عليه وآله وسلم)

((علم لا ينفق به ككنز لا ينفق منه))

حديث شريف

*Dedication*  
*I dedicate this effort to*  
*My*  
*Late Father*  
*My Mother*  
*My Brother, My Sister, and*  
*For the person which filled my heart by hope*  
*every day*

### Supervisor's Certification

We certify that this thesis was prepared under our supervision at Al – Nahrain University as a partial requirement for the Degree of Master of the Science in physics.

Signature :



Name : Dr. Mazin F. Mahrok

Title : Assistant Professor

Address : Department of Physics,  
College of Science,  
Al-Nahrain University.

Date : 2/ 8 / 2010

Signature :



Name : Dr. Thamir A. Jumah

Title : Lecturer

Address : Department of Physics,  
College of Science,  
Al-Nahrain University.

Date : 3/ 8 / 2010

In view of the available recommendation, I forward this thesis for debate by the examination committee.

Signature:



Name : Dr. Ahmad K. Ahmad

Title : Assistant Professor

Address : Head of Physics Department  
College of Science,  
Al-Nahrain University.

Date : 8/ 8 / 2010

## Committee Certification

We certify that we have read the thesis entitled (*X-ray Radiographic Study of Simulated Voids –Like Defects in Aluminum Casting and Welded Joints in Steel*) and as examining committee examined the student (*Farqad Rasheed Saeed*) in its contents and that in our opinion meets the standard of thesis for the degree of Master of Science in physics .

Signature:



Name: Dr. Emad K. Al-Shakarchi

Title: Assistant Professor

Address: Al-Nahrain University

Date: 13/12/2010

{Chairman}

Signature:



Name: Dr. Nabil N. Rammo

Title: Assistant Professor

Address: University of Baghdad

Date: 14/12/2010

{Member}

Signature:



Name: Dr. Abdul Hadi K. Judran

Title: Assistant Professor

Address: University of Technology

Date: 19/12/2010

{Member}

Signature:

Name: Dr. Mazin F. Mahrok

Title: Assistant Professor

Address: Al-Nahrain University

Date: / / 2010

{Supervisor}

Signature:



Name: Dr. Thamir A. Jumah

Title: Lecturer

Address: Al-Nahrain University

Date: 19/12/2010

{Supervisor}

Approved by University, Committee of Graduate Studies

Signature:

Name: Dr. Laith Abdul Aziz Al-Ani

Title: Assistant Professor

Address: Dean of College of Science / Al- Nahrain University

Date: / / 2010

## **ACKNOWLEDGMENT**

*First of all, profusely and all thanks are due to ALLAH, lord of the whole work creation who enabled me to achieve this work.*

*I wish to express my sincere thanks and gratitude to my supervisors: Dr. Mazin F. Mahrok and Dr. Thamir A. Jumah for suggesting this project, help, guidance, and advice, throughout the period of this work and for many helpful discussions and suggestions.*

*My thanks are extended to the head of Physics Department, and the staff of the department for their kind attention.*

*Thanks are also due to Mr. Hayder Thamir for providing necessary materials and x-ray radiography tools.*

*Special thanks are due to the Dr. Abdulhadi K. Jedran, and to all who helped me to achieve this work.*

*I am also very grateful to the General Company for Heavy Engineering Equipments and for Mr. Laith Sami for his help.*

*Finally, special words of thanks are also extended to my family, for their patience, understanding and acceptance of my preoccupation with this work.*

*Farqad*

## Summary

This project investigates the detection and evaluation of imperfections in internal structures of castings and welded joints by x-ray radiography. Optimum radiography conditions that lead to clear and high contrast image on the radiograph were studied.

Equations derived earlier for finding the size and depth of defects in castings were used in this project to test their applicability to a wide range of geometrical parameters used in radiography.

The importance of non-destructive testing NDT in industry is discussed. X-ray radiography being one of the NDT techniques, has some privilege over other techniques. For example, welded joints sometimes contain internal flaw or blowholes that may escape detection by other NDT techniques but can not escape detection by x-rays.

Two kinds of samples are prepared for radiography. The first sample is aluminum casting through which two different sizes of steel spheres are included. This sample was radiographed from two opposite sides and the x-ray films were analyzed. The second sample is steel plates which are welded by arc welding and then radiographed by x-rays. Imperfections in this sample such as incomplete root penetration, undercut and porosity were detected by x-ray radiography.

Different conditions influencing the preparation and radiography of the above samples were studied. The prepared welded sample was radiographed three times for different high voltages (120,140,160) kV respectively with an exposure time of (80) second. The best quality image where the defects can be detected clearly if its size is (5%) of the radiographed object using (120) kV and (140) kV. Moreover the results show that the optimum film gradient was found at (140)kV and the

contrast is better than obtained with (120)kV while darkening image was found at (160)kV.

In field of the aluminum casting, the two equations were derived earlier proved their capabilities as a right method for identification each of size and depth of such defects in castings and welded joints.



## *List of Contents*

<b>No.</b>	<b>Content</b>	<b>Page</b>
	<b>Chapter One</b> <b>Introduction</b>	
<b>1.1</b>	<b>Introduction</b>	<b>1</b>
<b>1.2</b>	<b>The Cause of Abnormalities in Brief as Follows</b>	<b>1</b>
<b>1.3</b>	<b>Evaluation of Welds</b>	<b>2</b>
<b>1.4</b>	<b>Defects in Welding</b>	<b>2</b>
<b>1.4.1</b>	<b>Surface Imperfection</b>	<b>2</b>
<b>1.4.2</b>	<b>Internal Defects</b>	<b>3</b>
<b>1.5</b>	<b>Evaluation of Castings</b>	<b>5</b>
<b>1.6</b>	<b>Defects in Castings</b>	<b>5</b>
<b>1.7</b>	<b>Diagnosis of Abnormalities</b>	<b>7</b>
<b>1.7.1</b>	<b>Destructive Tests (DT)</b>	<b>7</b>
<b>1.7.2</b>	<b>Non Destructive Tests (NDT)</b>	<b>7</b>
<b>1.7.2.1</b>	<b>Visual Inspection</b>	<b>8</b>
<b>1.7.2.2</b>	<b>Liquid Penetrates Inspection</b>	<b>8</b>
<b>1.7.2.3</b>	<b>Magnetic Particle Inspection</b>	<b>9</b>
<b>1.7.2.4</b>	<b>Eddy Current Inspection</b>	<b>9</b>
<b>1.7.2.5</b>	<b>Ultrasonic Inspection</b>	<b>9</b>
<b>1.7.2.6</b>	<b>Radiography Inspection</b>	<b>10</b>
<b>1.8</b>	<b>Production of X-ray</b>	<b>11</b>
<b>1.8.1</b>	<b>Absorption and Attenuation of X-ray</b>	<b>12</b>

<b>1.8.2</b>	<b>Geometric Unsharpness</b>	<b>13</b>
<b>1.8.3</b>	<b>X-ray Film</b>	<b>14</b>
<b>1.8.3.1</b>	<b>Development</b>	<b>15</b>
<b>1.8.3.2</b>	<b>Fixation</b>	<b>15</b>
<b>1.8.4</b>	<b>The "speed" of The Film</b>	<b>15</b>
<b>1.8.5</b>	<b>Radiographic Contrast</b>	<b>16</b>
<b>1.8.6</b>	<b>The Characteristic Curve</b>	<b>17</b>
<b>1.8.7</b>	<b>Radiographic Sensitivity</b>	<b>18</b>
<b>1.9</b>	<b>Method of Identification of Foreign Materials in Casting or Welding by Using X-ray Radiography</b>	<b>19</b>
<b>1.10</b>	<b>Literature Review</b>	<b>21</b>
<b>1.11</b>	<b>Aim of the Work</b>	<b>24</b>
	<b>Chapter Two Experimental Part</b>	
<b>2.1</b>	<b>Introduction</b>	<b>25</b>
<b>2.2</b>	<b>Samples Preparations</b>	<b>25</b>
<b>2.2.1</b>	<b>Steel Plates</b>	<b>25</b>
<b>2.2.2</b>	<b>Casting Sample</b>	<b>26</b>
<b>2.2.3</b>	<b>Welded Sample</b>	<b>28</b>
<b>2.3</b>	<b>Nondestructive Testing</b>	<b>29</b>
<b>2.3.1</b>	<b>X-ray System</b>	<b>29</b>
<b>2.3.2</b>	<b>X-ray Film</b>	<b>30</b>
<b>2.3.3</b>	<b>Optical X-ray Film Density</b>	<b>31</b>
<b>2.3.4</b>	<b>Geometric Image Unsharpness</b>	<b>32</b>

<b>2.3.5</b>	<b>Characteristic Curves of X-ray Film</b>	<b>32</b>
<b>2.3.6</b>	<b>Sensitivity Tests for Radiography of Welded Sample</b>	<b>33</b>
<b>2.3.7</b>	<b>Measurement of Film Density</b>	<b>34</b>
<b>2.4</b>	<b>Identification of Foreign Materials in Casting by Using X-ray Radiography</b>	<b>35</b>
	<b>Chapter Three</b> <b>Results and Discussions</b>	
<b>3.1</b>	<b>Introduction</b>	<b>36</b>
<b>3.2</b>	<b>Geometric Image Unsharpness Result</b>	<b>36</b>
<b>3.3</b>	<b>Optical Density Measurements and Calculations</b>	<b>37</b>
<b>3.4</b>	<b>Defect Interpretation for Welded Sample</b>	<b>39</b>
<b>3.4.1</b>	<b>Sensitivity Determination for Welded Sample</b>	<b>42</b>
<b>3.4.2</b>	<b>Characteristic Curves of X-ray Film</b>	<b>42</b>
<b>3.4.3</b>	<b>Correlation between Characteristic Curves and Welded sample Contrast at Different (kV) and Sensitivity</b>	<b>46</b>
<b>3.5</b>	<b>Defects Interpretation for Casting Sample</b>	<b>47</b>
<b>3.5.1</b>	<b>Identification of Foreign Materials</b>	<b>50</b>
	<b>Chapter Four</b> <b>Conclusions and Future Work</b>	
<b>4.1</b>	<b>Conclusions</b>	<b>54</b>
<b>4.2</b>	<b>Future Work</b>	<b>55</b>
	<b>References</b>	<b>56</b>

## *List of Symbols*

<b>Symbol</b>	<b>Definition</b>
<b>dI</b>	<b>Loss a part of x-ray beam intensity</b>
<b><math>\mu_m</math></b>	<b>Mass absorption coefficient</b>
<b>I</b>	<b>Emergent intensity of x-ray</b>
<b>I<sub>o</sub></b>	<b>Incident intensity of x-ray</b>
<b><math>\mu</math></b>	<b>Linear absorption coefficient</b>
<b><math>\rho</math></b>	<b>Density of material</b>
<b>D</b>	<b>Optical film density</b>
<b><math>\gamma</math></b>	<b>Film gradient</b>
<b>C</b>	<b>Contrast</b>
<b>E</b>	<b>Exposure factor</b>
<b>U<sub>g</sub></b>	<b>Geometric image unsharpness</b>
<b>X</b>	<b>Thickness of sample</b>
<b>F</b>	<b>Focal spot size</b>
<b>L</b>	<b>Focal Object Distance(F.O.D)</b>
<b>IQI</b>	<b>Image quality indicator</b>
<b>t</b>	<b>Exposure time</b>
<b>Y</b>	<b>Depth of steel sphere</b>
<b>R</b>	<b>Actual radius of steel sphere</b>
<b>R<sub>R</sub></b>	<b>Radius of the steel spheres on radiograph when the casting is radiographed from side (R)</b>
<b>R<sub>L</sub></b>	<b>Radius of the steel spheres on radiograph when the casting is radiographed from side (L)</b>

**Chapter One**

**Introduction**

## Chapter One

### 1.1 Introduction

Not all industrial components that are manufactured meet the required specification. Defects of many types and sizes may be introduced to a component either in casting or welding during manufacture and the nature and size of many defects may influence the subsequent performance of the component. Other defects, such as imperfections or corrosion may be generated within a material during service. It is therefore necessary to have reliable means for detecting the presence of defects at the manufacturing stage and during the performance of that component. Inspection systems (visual or nonvisual) using well-established physical principles have been developed which will provide information on the quality of a component and which will not alter or damage the components or assemblies <sup>[1]</sup>.

Accordingly the benefits of inspection of manufactured component can be divided into three categories <sup>[2]</sup>.

1. Increased productivity.
2. Increased serviceability.
3. Safety.

### 1.2 The Cause of Abnormalities in welded joints and castings

1. Inherent defects - introduced during the initial production of the base or raw material.
2. Processing defects - introduced during processing of the material or part.
3. Service defects - introduced during the operating cycle of the material or part <sup>[2]</sup>.

### 1.3 Evaluation of arc Welds

Welding processes are widely used in the fabrication of nearly all industrial components. Despite the best care taken during design and fabrication, many of the welded components fail especially at the weld joint and heat affected zones, drastically influencing the performance reliability. Many failures are attributed to improper design of weld joint, bad preparing the surfaces being welded, selection of base materials and filler material, welding processes, and operating parameters .One way to minimize the failures of welded components is to apply non-destructive testing (NDT) procedures immediately after the fabrication to make sure that the welded joint is defect-free <sup>[3]</sup>.

Data on defect dimensions help fracture mechanics to assess the health of welded component <sup>[4]</sup>.

### 1.4 Defects in Welding

#### 1.4.1 Surface Imperfection

1. Pitting refers to imperfections appearing on the surface of the parent metals, usually in the form of small depression, and is caused by corrosion or the lifting of scale during rolling of plate material <sup>[5,6,7]</sup>.

2. Weld spatters are imperfections appearing on the surface of the weld or parent metals formed by globules of metal expelled during arc-welding. This is an inherent property of some electrodes, but may be caused by excessive welding current .Weld spatter can be dangerous as the adherence is generally poor and so is liable to become detached during service <sup>[5,6,7]</sup>.

3. Chipping, peening, or grinding marks are surface indentations due to chased cuts. They are caused by incomplete dressing of the weld area. If a grinding groove is narrow and of sufficient depth it may be dangerous and

its radiographic appearance will probably be similar to that of an internal weld defects<sup>[5,6,7]</sup>.

4. Under cutting is a groove or channel in the surface of the plate along the edge of the weld. It can occur when the electrode held at incorrect angle with excessive current. This may materially reduce the joint strength particularly<sup>[5,6,7]</sup>.

5. Incompletely filled groove is a continuous or intermittent channel. It is a butt weld face where the thickness of the throat is less than that of the parent. It is caused by failure to fill up the crater with weld metal<sup>[5,6,7]</sup>.

6. Excessive penetration is an excess of weld metal protruding through the root in a fusion butt weld. An excessive penetration can be unacceptable especially in pipe welds by causing an impediment to fluid flow<sup>[5,6,7]</sup>.

7. Exposed inclusions or exposed porosities are slag or other foreign material entrapped during welding and appearing partly on the weld surface, giving a pit or pock mark at the surface of the weld<sup>[5,6,7]</sup>. However, these inclusions may not appear on the weld surface.

8. Overlap is an imperfection at the toe or root of a weld caused by an over flow of weld metal on the surface of the parent metals with out fusing with the latter. It is caused when the welding rod has been used at incorrect angle, the electrode has traveled too slowly, or the current was too low<sup>[5,6,7]</sup>.

#### **1.4.2 Internal Defects**

1. Blowholes, voids, or gas bubbles are large cavities resulting from gas being entrapped in the weld. The term blowholes are caused by damp electrodes or too high a current or high speed of electrode or possible lamination or corrosion of parent metal or greasy or painted plate edges . A blowhole will not seriously affect the mechanical properties of a weld unless its size is excessive<sup>[5, 6, 7]</sup>.



2. Pipe is an elongated or tubular cavity in the weld metals due to entrapped gas. Capillary pipe is a fine pipe extending along the junction of a weld and parent metal. The cause of a pipe is generally similar to that for a blowhole, but it is frequently due to moisture in the electrode coating. Capillary pipes are normally due to faults in the parent metal <sup>[5,6,7]</sup>.

3. Porosity: this occurs when gases are trapped in the solidifying weld metal. These may arise from dirt, particularly oil or grease, on the metal in the vicinity of the weld. This can be avoided by performing the process in completely dry condition <sup>[5,6,7]</sup>.

4. Incomplete root penetration is a lack of fusion in the root of weld or a gap left by the failure of the weld metal to fill the root of a butt weld. It is caused by the electrode held at an incorrect angle, too large in diameter, travel too fast, an insufficient welding current, or an improper joint preparation. Incomplete root penetration can form serious defects, as the unfused area permits stress concentration and may initiate cracking <sup>[5,6,7]</sup>.

5. Lack of fusion describes the failure to fuse together adjacent layers of weld metal or adjacent weld metal and parent. The defect results mainly from the presence of slag, oxides, or other nonmetallic substances, too low a welding current, incomplete fusion and it can also arise from too high welding speed. The defect reduces the strength of the joint, and under cyclic or shock loading it is serious <sup>[5,6,7]</sup>.

6. Slag inclusions, and other nonmetallic inclusions, may be the result of weld-metal contamination by substances on the surface of the joint, or by the atmosphere, but the usual source is the slag formed by the electrode covering. The slag inclusions are often associated with lack of penetration and under cut that may occur in between weld runs. Occurrence of large irregular inclusions will reduce the strength of a weld. The presence of small isolated inclusions may not affect the strength of welded structures, but may

be considered adverse to design when included in high pressure pipe runs<sup>[5,6,7]</sup>.

7. Cracks can occur in either the weld metal or parent metals. In the former they are classified as longitudinal or transverse. In the latter it is in the parent plates with the origin in the heat-affected zone of the weld. Weld metal cracks are caused by high localized stresses in the joint arising from the shrinkage of weld metal, or by resistance of movement of the parent or by vibration of the structure during welding. Therefore it is important that each weld run is strong enough to withstand the shrinkage and to allow as much freedom of movement as possible<sup>[5, 6, 7]</sup>.

## 1.5 Evaluation of Castings

Castings may contain certain imperfections which contribute to a normal quality variation. Such imperfections are taken as defects or flaws only when they affect the appearance or the satisfactory functioning of the castings and the castings in turn do not come up to the quality and inspection standards being applied. Defective castings offer an ever-present problem to the foundry industry. Defective castings account for the normally higher losses incurred by the foundry industry. Casting defects are usually not accidents, they occur because step in the manufacturing cycle does not get property controlled. A defect may be the result of a single clearly defined cause or of a combination of factors in which case necessary preventive measures are more important<sup>[8]</sup>.

## 1.6 Defects in Castings

There are several known defects introduced in the castings as in the following:

1. Porosity or gas-holes are spherical holes of varying size, with bright walls, distributed in the metal. The larger holes tend to be found in the heavier sections (last to be solidified). The gas in the molten metal is removed by keeping casting ladles and moulds dry<sup>[5, 9,10]</sup>.

2. Blowholes are mainly found in two forms.

A- Elongated cavities with smooth walls. Found just below the surface of the topmost part of a casting. These are caused by entrapped air and can be avoided by venting the mould<sup>[5, 9,10]</sup>.

B- Rounded shape cavities with smooth bright walls are caused by mould gases coupled with insufficient permeability, or venting. They can be avoided by using less oil binder in the mould and ensuring core is dry<sup>[5, 9,10]</sup>.

3. Inclusion these are material discontinuities formed by the inclusion of oxides, dross, sand and slag in a casting. They are due to careless skimming and pouring, to the use of a dirty ladle, and to turbulence. This can be avoided by proper use of equipment and foundry practice<sup>[5,11]</sup>.

4. Hot tears are a discontinuity caused by fracture of the metal during its contraction as it cools during the early stages after solidification. They appear as one or more dark spots, jagged and lines on radiographic films<sup>[5,12]</sup>.

5. Shrinkage a casting defect that occurs during the middle and later stages of solidification of the cast metal. It is a form of void and can be distinguished from that of sponginess<sup>[5, 9,10]</sup>.

6. Cracks are well defined and normally straight features; they are formed after the metal has become completely solid. High thermal stress is required to cause fracture<sup>[5, 13]</sup>.

7. Cold shuts: these are discontinuities (a form of lack of fusion) caused by the failure of a stream of molten metal to unite with another stream of metal, or with a solid metal section such as a chaplet. They are linear in appearance. With perhaps a curling of the molten in the mould will appear as a dark crescent or circle<sup>[5]</sup>.

8. Unfused chaplet: a chaplet is often used to support a section of a mould and where the molten metal is poured in; the chaplets should fuse into the casting. When unfused the chaplet will cause a discontinuity in the casting design <sup>[5]</sup>.

9. Misplaced core: is an irregularity of wall thickness. One wall thicker than the other and can be detected by radiography technique <sup>[5]</sup>.

10. Segregation: this discontinuity comprises particular component of the metal composition that have different solidification temperatures. And so tend to be driven by solidifying metal and segregate at particular area, particularly the central zone of a casting. This may appear as light or dark area in radiographic films <sup>[14]</sup>.

## 1.7 Diagnosis of Abnormalities

The diagnosis of abnormalities can be classified into two major groups.

### 1.7.1 Destructive Tests (DT)

Tests are carried out to evaluate the specimen in order to understand a specimen's structural performance or material behavior under different loads. Also to find out how strong, flexible, or long-lived a material is often requires the ultimate sacrifice: the destruction of the sample by equipments designed to precisely measure its performance in the face of a force. Mechanical techniques and some of chemical analysis are wide known of (DT) techniques <sup>[8]</sup>.

### 1.7.2 Non Destructive Tests (NDT)

During recent years the use of non-destructive testing of material components and assemblies has grown to a great extent, together with a similar growth in the use of mass-production methods <sup>[15]</sup>.

NDT refers to all the test methods which permit testing or inspection of material without impairing its future usefulness<sup>[16]</sup>.

Non destructive evaluation NDE procedure plays an important role in materials processing, as well as in subsequent materials testing, product design, manufacturing and quality control of manufactured products. They are also essential to the integrity of structural elements and complex system. Accept or reject criteria should be based on NDE, critical safety efficiency and operational features of large scale structures depend on adequate NDE capabilities<sup>[17]</sup>.

### **1.7.2.1 Visual Inspection**

Visual inspection methods are intended to detect the surface discontinuities and may be carried out with naked eye or by using a magnifying glass.

Generally visual inspection is used to determine such things as the surface, shape or evidence<sup>[18]</sup>.

### **1.7.2.2 Liquid Penetrates Inspection**

Non-destructive method for finding discontinuities that is open to the surface of solid and essentially non porous materials<sup>[19]</sup>. This inspection depends mainly on a liquids penetrant (developer and penetrant). The developer is effectively wetting the surface of solid specimen and the penetrant must have the ability to enter extremely fine surface defects. Red is the most commonly used color in dye penetrants and this color is the most readily seen by human eye<sup>[1]</sup>. The technique is simple, low cost, portable, and results easily interpreted. The limitations of this technique are that the defect must be open to the surface and can not employ for porous materials<sup>[20]</sup>. This technique is just for use to metal or alloy materials especially for welded joints.

### 1.7.2.3 Magnetic Particle Inspection

Magnetic particle inspection is sensitive method of locating surface and some sub-surface defect in ferromagnetic component. The basic principle of this method is that while magnetic flux line are caused to flow in a sample, the local disturbance at flow is detected by using magnetic powder either dry or preferably as a suspension in a liquid<sup>[1,15, 21]</sup>.

The advantages of this method are fast, low cost and possible to obtain good indication even if a sample contains contaminating material. The disadvantages of this method are restricted of ferromagnetic materials and restricted to surface or near surface flaws.

### 1.7.2.4 Eddy Current Inspection

Eddy current inspection is based on the principles of electromagnetic induction and it is used for electrically conductive material<sup>[19]</sup>.

If a coil carrying an alternating current is placed in proximity to a conductive material, secondary or eddy current will be induced within the material. The induced currents will produce a magnetic field which will be in opposition to the primary magnetic field surrounding the coil. The impedance of a coil can be determined by measuring the voltage across it. Eddy current test equipment, change in coil impedance can be indicated on a meter or display on the screen. The advantages of this technique are high speed, low cost and no contact required. It was used for inspecting the conductive material only<sup>[1,19]</sup>. The disadvantage of this technique are wide range of parameters which affected the eddy current responses and generally tests restricted to surface breaking conditions and slightly subsurface flaws.

### 1.7.2.5 Ultrasonic Inspection

The imaging of materials discontinuities by ultrasound depends in part on the difference in acoustic impedance of two adjacent materials. Most

ultrasonic inspection is performed at frequencies between (1) and (25) MHz<sup>[22, 23]</sup>. The electrical pulse is applied to a piezo electric transducer which converts electrical to mechanical energy and other wise is valid. The ultrasonic energy levels through the material at a specific velocity that depends on the physical properties of the material. The amount of energy reflected from or transmitted through an interface or other type of discontinuity, dependent on the properties of reflector<sup>[1]</sup>. The advantage of this technique is its capability for inspection of thick section (up to 2meters), low cost, and portable and can be used for great variety of materials<sup>[6]</sup>. The disadvantages of this technique are calibration blocks required, also the technique requires smooth surface, and no permanent record, but possible with more complex computer based analysis<sup>[22]</sup>.

#### 1.7.2.6 Radiography Inspection

Radiography is a well established NDT method for obtaining information about discontinuity through out the specimen<sup>[25]</sup>. Radiography is performed by placing photographic film mounted in light-tight holder as close to object as possible and then irradiating the assembly from the opposite side with either x-ray or  $\gamma$ -ray<sup>[24, 26]</sup>. Radiography is a very useful NDT system; the term radiography is a process in which an image is produced on film. Radiography is capable of detecting any feature in a structure provided that there are sufficient differences in thickness or density within the test piece. Radiography method is generally used for the successful detection of internal flaws that are located beneath the surface<sup>[1]</sup>.

The interaction of x-ray enables part to be inspected by differential attenuation of radiation intensity. The most features of radiography technique are:

Detection of internal defects, surface defects, can be used for many materials, and the correctness of part assemblies. On the other hand the

limitation of radiography technique is the maximum materials thickness, and on the smallest imperfection that can be detected by x-ray

## 1.8 Production of X-rays

X-rays are produced when an energetic beam of electrons is suddenly arrested by impinging upon a target. By thermionic emission, electrons come from electrically heated filament of tungsten, and are allowed to hit a block of high atomic number material. Both of the filament and the target are contained inside an evacuated glass tube. The spectrum of x-rays, when examined, is found to be composed of two parts due to two different mechanisms. Fig.(1.1) shows the interaction between electrons and target atoms in x-ray tube.

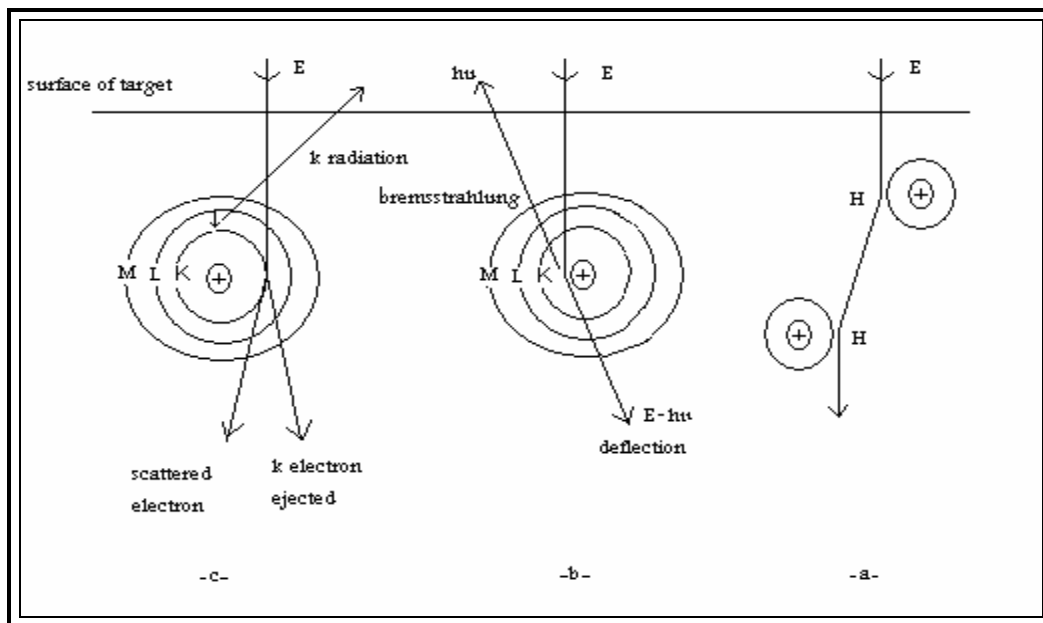


**Fig.(1.1) Interaction between electrons and target atoms in x-ray tube<sup>[27]</sup>**

Electron – a – approaches the atom and will be repelled, deflected and slowed down. The target material gains energy, it is heated up.

Electron – b – penetrates through the atom and approaches the nucleus. It suffers a change in direction and large reduction in its speed and energy. The



energy lost by the electron is emitted as x-ray. This ray is called bremsstrahlung which means braking radiation also called continuous x-ray. Electron – c – interacts with an individual electron in the atom. The orbital electron is removed from the shell. The result is ionization of target atom. The vacancy is filled from another shell and characteristic x-rays may be emitted<sup>[27]</sup>.

### 1.8.1 Absorption and Attenuation of X-ray

When an x-ray beams of intensity (I) passes through a material of thickness (dx) it loses a part (dI) of its intensity.

$$dI = - \mu_m I dx \quad \dots\dots\dots (1.1)$$

Consequently we come to the exponential law of absorption, written as

$$I = I_0 \exp (- \mu_m \rho x) \quad \dots\dots\dots (1.2)$$

$$\mu_m = \mu / \rho \quad \dots\dots\dots (1.3)$$

Where  $\rho$  is the density of the material in  $g / cm^3$  and  $\mu_m$  is termed as mass absorption coefficient, in  $cm^2 / g$  which is independent of thickness (x). And is a function of the energy of the absorbed radiation and the atomic number of the absorbing element.

$$(\mu / \rho) \propto Z^m / E^n$$

where m is a number between 4 and 5

n is a number between 2 and 3

In the case of homogeneous material the above equation will be<sup>[32]</sup>.

$$I = I_0 \exp (- \mu x) \quad \dots\dots\dots (1.4)$$

Where  $I$ ,  $I_0$  are the emergent and incident intensities respectively .

$\mu$ : Linear absorption coefficient expressed in units of  $\text{cm}^{-1}$

$X$ : is the thickness of the absorber in cm.

### 1.8.2 Geometric Unsharpness

Geometric unsharpness refers to the loss of definition as a result of geometric factors of the radiographic equipment and setup. It occurs because the radiation does not originate from a single point but rather over an area<sup>[28]</sup>. Fig.(1.2) shows two sources of different sizes, the paths of the radiation from each edge of the source to each edge of the feature of the sample, the locations where this radiation will expose the film and the density profile across the film. Image (a), the radiation originates at a very small source. Since all of the radiation originates from basically the same point, very little geometric unsharpness is produced in the image. Image (b) , the source size is larger and the different paths that the rays of radiation can take from their point of origin in the source causes the edges of the notch to be less defined.

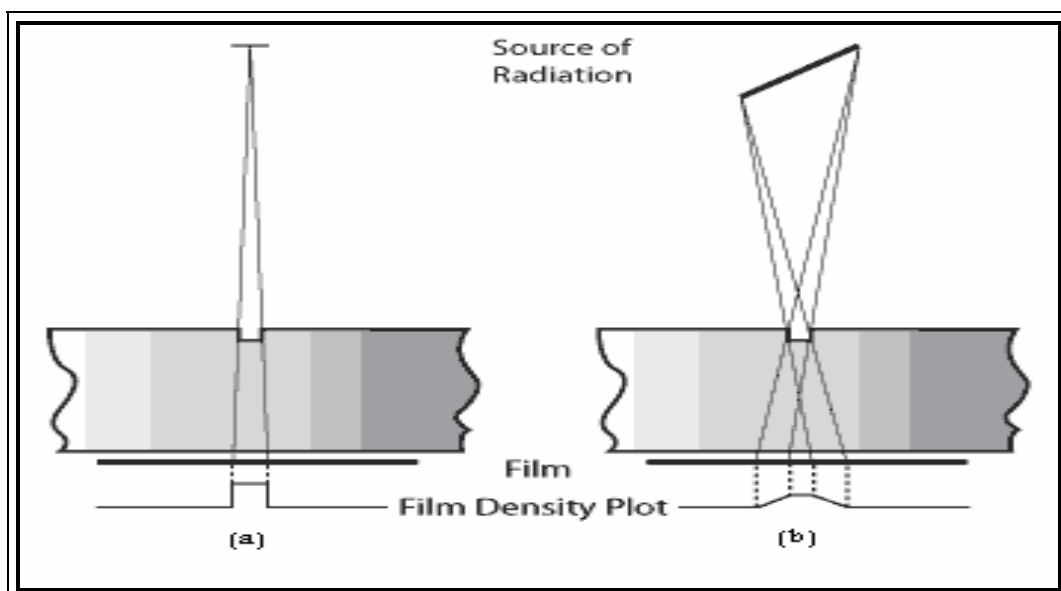


**Fig. (1.2) Schematic diagram showing geometric image unsharpness**

(Ug)

The three factors controlling unsharpness are source size, source to object distance, and object to film distance <sup>[29]</sup>. The source size is obtained by referencing manufacturer's specifications for a given x-ray or gamma ray source. Industrial x-ray tubes often have focal spot sizes of 1.5 mm squared. As the source size decreases, the geometric unsharpness also decreases. For a given source size, the unsharpness can be decreased by increasing the source to object distance, but this comes with a reduction in radiation intensity. The object to detector distance is usually kept as small as possible to help minimize unsharpness. The area of varying density at the edge of a feature that results due to geometric factors is called the penumbra. The penumbra is the gray area seen in fig. (1.2) (b). Code and standards used in industrial radiography require that geometric unsharpness be limited. It is difficult to measure it exactly in a radiograph. Therefore it is typically calculated. The source size must be obtained from the equipment manufacturer. Then the unsharpness can be calculated using measurements made of the setup. The following formula is used to calculate the maximum amount of unsharpness (**U<sub>g</sub>**) due to specimen thickness<sup>[30]</sup>.

$$U_g = F \times X/L \quad \dots\dots\dots (1.5)$$

F = Source focal-spot size

L = Distance from the source to front surface of the object

X = The thickness of the object

### 1.8.3 X-ray Film

It is constructed from a film base usually made of cellulose tri-acetate which is relatively thick and transparent layer. The film base is surrounded by two layers of emulsion and hence the film is called double-coated film. In the emulsion layers all the changes occur which result in the production of the visible pattern. The emulsion layers consist of gelatin in which is

suspended a very large number of tiny crystals of silver bromide. The emulsion layers are attached to the film base by very thin layers of gelatin plus a solvent for cellulose tri-acetate. Finally, two super coating layers, which consist of clear gelatin, cover the x-ray film from both sides. When x-rays penetrate the protective plastic cover of the cassette, they cause the intensifying screen to convert a few absorbed x-ray photons into a lot of light photons<sup>[31]</sup>.

### 1.8.3.1 Development

During which the affected silver bromide crystal are converted into opaque, black silver spots, whilst those which have not been sufficiently affected remain in their previous yellowish translucent state<sup>[31]</sup>.

### 1.8.3.2 Fixation

The unaffected AgBr crystals are dissolved away, leaving only the record of the x-ray pattern in the form of black silver spots embedded in gelatin. After fixation the film should be washed to remove the processing chemicals as well as the products of the chemical reaction during processing. The final step is to dry the film<sup>[31]</sup>.

### 1.8.4 The "speed" of The Film

The exposure which is needed to produce a density ( $D = 1$ ) depends upon a type of film. If a small exposure is needed, then the film is "fast" where as if a large exposure is needed then the film is "slow". Fig. (1.3) shows characteristic curves of two films. Film (A) is 'faster' than film (B), i.e., film (A) needs a smaller exposure for the same optical density as compared to film (B)<sup>[31]</sup>.

$$E = I t \quad \dots\dots\dots (1.6)$$

E: Exposure in roentgens

I: Intensity in roentgens/sec

t: Exposure time in sec

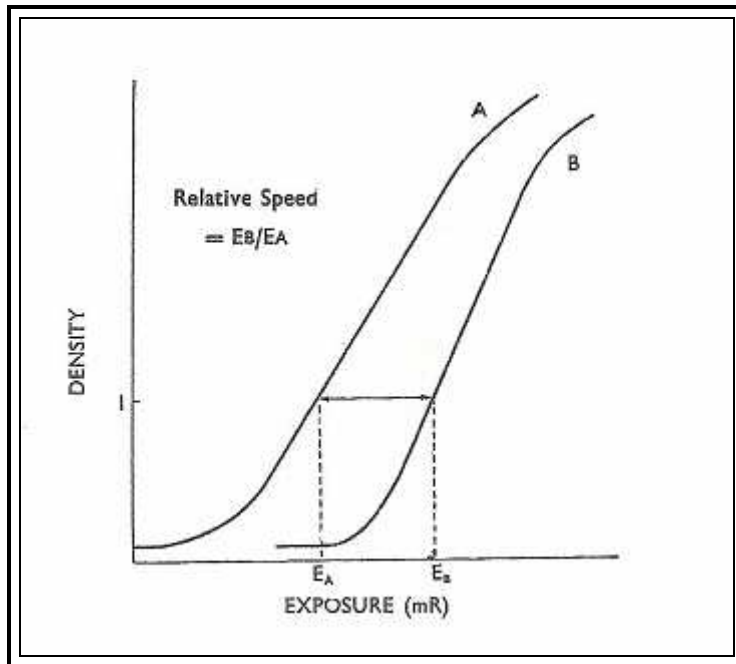


**Fig. (1.3)The characteristic curves of two films. Film (A) is ‘faster’ than film (B), i.e., needs a smaller exposure for the same density <sup>[31]</sup>**

### 1.8.5 Radiographic Contrast

The density difference on a radiograph between an image and the background is known as contrast.

The blackening of the x-ray film is measured by means of a quantity which is known as optical density.

$$\text{Optical density} = \log_{10} (I_0/I) \quad \dots\dots\dots (1.7)$$

Where ( $I_0$ ) is intensity of visible light incident upon a small area of the film and ( $I$ ) is the intensity of light transmitted from that small area .

The contrast ( $C$ ) is defined by

$$C = D_2 - D_1 \dots\dots\dots (1.8)$$

Where  $D_2$  and  $D_1$  are optical densities at two points. The minimum detectable contrast that a human eye can see is a bout  $0.02^{[32]}$ .

### 1.8.6 The Characteristic Curve

It reveals the behavior of the x-ray film with the quantity of x-ray radiation striking it.

Fig. (1.4) shows the characteristic curve of an x-ray film from this figure the fog level (ab) which is represented by the background low density region is always present and added to the density resulting from the exposure. Range of visual densities is (0.25 to 2.5).

Also from the figure. (1.4) the straight line portion (cd) represents the most important region of the film. In this range of exposures; the density is proportional to the logarithm of the exposure. Since the eye responds to contrasts (that is difference in density) it is important to consider the difference in density brought about by different exposures.

Therefore, the physiological response of the eye to visible light of different intensities is logarithmic. The slope ( $\gamma$ ) measures the maximum density difference resulting from two exposures.

Film ( $\gamma$ ) equals

$$\gamma = (D_2 - D_1) / (\log_{10} E_2 - \log_{10} E_1) \dots\dots\dots (1.9)$$

$D_2$  and  $D_1$  are the densities which result from exposure of  $E_2$  and  $E_1$  respectively <sup>[31]</sup>.

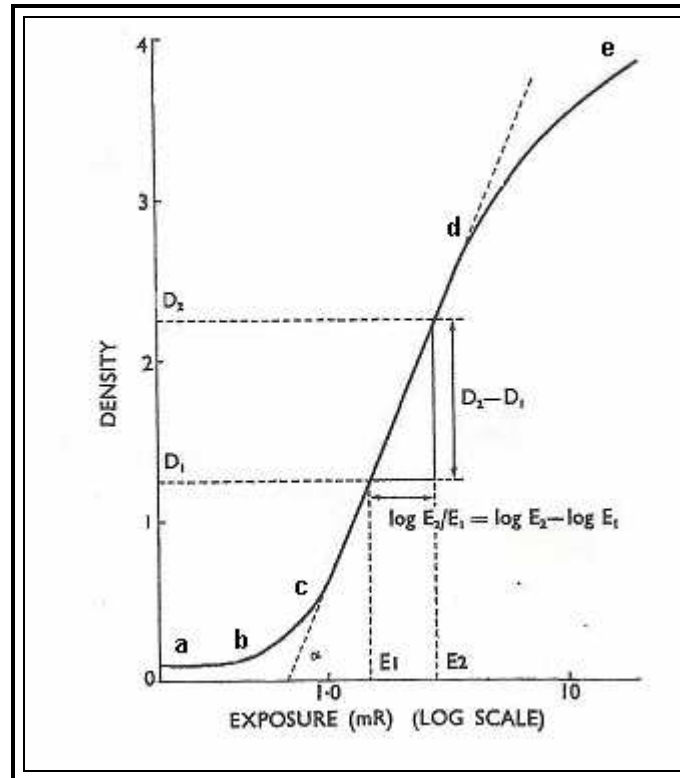


Fig. (1.4) The characteristic curve of an x-ray film <sup>[31]</sup>

### 1.8.7 Radiographic Sensitivity

The ability to detect a flaw in the specimen depends on the nature of the flaw, its shape and orientation to the radiation beam as well as on the film selection, geometrical unsharpness, and film density <sup>[21]</sup>. Image quality indicator (IQI) sensitivity is not directly a measure of flaw sensitivity. The step, wire and holes types of penetrameter will not give the same sensitivity value when used under identical conditions <sup>[15]</sup>. The wire and hole (IQI) type penetrameter consists of sets of wires arranged in increasing order of diameters (0.032 to 3.2 mm) <sup>[33]</sup>. The hole (IQI) type penetrameter consists of sets of holes arranged in increasing order of diameters (0.1 to 6.3 mm) <sup>[34]</sup>. The penetrameter shall be placed on the source side of the object being examined and should be placed so that the plane of the penetrameter is normal to the radiation beam, and the (IQI) sensitivity can be expressed as follows <sup>[35]</sup>.

Wire IQI sensitivity = (Diameter of smallest detectable wire) / (Thickness of specimen under wire) x 100 ..... (1.10)

Hole IQI sensitivity = (Diameter of smallest detectable hole) / (Thickness of specimen under hole) x 100 ..... (1.11)

## 1.9 Method of Identification of Foreign Materials in Casting or Welding by Using X-ray Radiography

In order to calculate the size and depth of defects and voids in objects, the following procedure was adopted. This involves taking two radiographs from two opposite sides of the object on two different x-ray films. By the analysis of x-ray films and the derivation of equation suitable for the experimental set up used, geometrical information about the defects may be obtained. Fig. (1.5) shows the parameters required to be measured in order to find the depth (Y) and the radius (R) of the defect inside the object.

If two separate radiographs are taken of the object, from two opposite sides as shown in fig. (1.5), then the actual values of (Y) and (R) could be calculated by considering the geometrical relationship of the radiographic parameters<sup>[36]</sup>.

$$Y = (R_R (L+X) - R_L L) / (R_R + R_L) \dots\dots\dots (1.12)$$

$$R = R_L R_R (2L+X) / ((L+X) (R_L + R_R)) \dots\dots\dots (1.13)$$

Special Case: If the defect is in the middle of the radiographed block, then the radii  $R_R$  and  $R_L$  on the radiographs are equal:

$$R_R = R_L$$

Substitute this result in equation (1.12) we get.

$$Y = X/2 \dots\dots\dots (1.14)$$



Put  $R_R = R_L$  in equation (1.13) we get.

$$R = R_L (2L+X) / (2(L+X)) \dots\dots\dots (1.15)$$

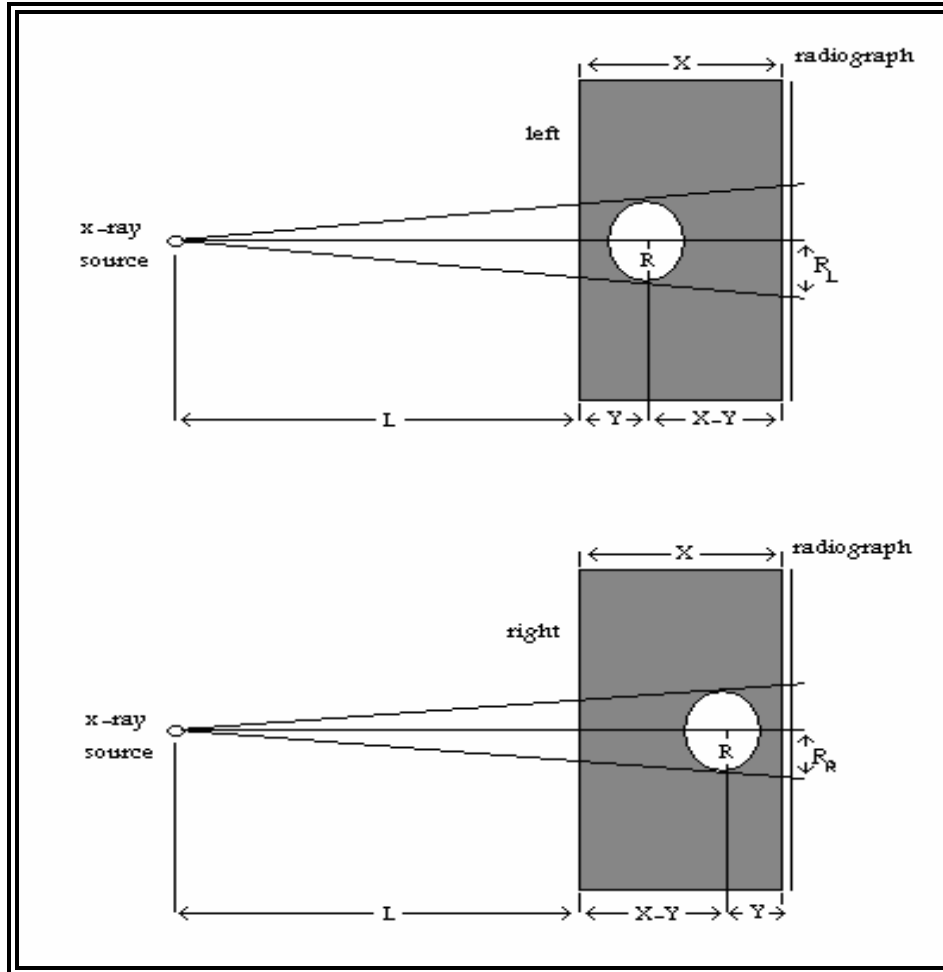


**Fig. (1.5) Experimental set-up for radiography showing the parameters used in equation (1.12) and (1.13) to calculate (Y) and (R) [36]**

## 1.10 Literature Review:

The art and science of Non-destructive testing NDT are very old. Probably one of the most famous and well known examples is that of Archimedes. In performing a test to determine if the king had been defrauded by the silversmiths. Archimedes discovered the principle that now bears his name.

In 1920, the non-destructive testing NDT has developed from a laboratory curiosity to non-destructive tool of production. However, the real revolution in NDT took place during world war II. The progress in materials engineering in identifying new and improved materials subsequent to a number of catastrophic failures in world war II like the brittle fractures of liberty ships, necessitated the requirement to test and improve material properties. This requirement resulted in a wider application of the existing NDT methods and techniques and also paved the way for development of new methods and techniques <sup>[37]</sup>. One of the most NDT techniques widely known is x-ray radiography.

X-ray was discovered by Rontgen in 1895. The establishment of the radiography after the discovery, added a unique dimension to man search for knowledge. The effect of radiography in the medical field has been tremendous. No less dramatic, has been the impact of x-ray on the engineering world where it is used as an inspection tool heralded a new era in NDT. Even up to the early 1950, industrial x-ray equipment was mainly modified medical equipment. In 1954, the description portable x-ray equipment has a very different meaning to that of today with equipment weighing up to 120 kg <sup>[38]</sup>.

In 1959 Hogarth published a paper on the use of x-radiography for examining defects in material as a common practice for many years <sup>[15]</sup>. In 1960, American welding society published a manual on radiography which is used to same extent for examination of brazed joints. As a general rule,

uniform thickness which is not too thick may be radiographed if an exposure can be made straight through the joint<sup>[39]</sup>.

In 1981 Huggins used 10 kV to 150 kV for radiography; he found that the energy region below 150kV resulted in radiographs which are free from scatter. This will not be so if the material being radiographed is of low atomic number<sup>[28]</sup>.

Development in radiography and Fluoroscopy in industrial field up to 1982 have been discussed by Stewart<sup>[40]</sup>.

Segal and Trichter in 1988 used radiography as a tool to estimate the width and depth of cracks. They concluded that the depth of the crack can not be determined without accurate information about the angle of exposure and the LSF (line spread function) of the radiography system<sup>[25]</sup>. In the same year Adams and Gawley<sup>[41]</sup> used x-ray radiography technique for inspection the composite (which contains steel mesh and bars and light weight of fiber reinforced) and bonded joints. They concluded that their design specifications of the composite used will often tolerate quite high levels of porosity (5% would be typical) and this is relatively simple to detect by x-ray radiography.

Also, Bushlin and Notea in 1988 concentrate on the study of typical rectangular crack and then estimated its size from the radiography. Their interpretation is based on a description of the radiographic image generation by the theoretical models<sup>[42]</sup>.

In 1990 Deutsch discussed inversion methods aimed at developing an inexpensive film in projection x-ray radiography. He used this method for the evaluation of cylindrically symmetric objects<sup>[43]</sup>.

In 2001 Jedran discussed Non destructive evaluation of ceramic \ metal joined systems by using x-ray radiographic technique. He found that the x-ray radiography technique is a suitable method for ceramic to metal lap

joining system and best operation condition for x-ray radiographic system must be determined <sup>[44]</sup>.

In 2001 Mahrok and Azeez found a practical method to calculate the size and depth of defects and voids in metals by the analysis of x-ray films and the derivation of the equations suitable for the experimental set up used <sup>[36]</sup>.

In 2003 Ayad studied the panoramic method of x-ray radiography for detection of welding defects in gas pipeline. The method was used to detect welding joints in pipes which are more than 10 inches in diameter <sup>[45]</sup>.

In 2006 Peter Hayward presents the results of various techniques used on selected samples. The used samples contained a variety of flaws and are subjected to radiographic inspection using x-ray, Ir 192 and Se 75. He also used different classes of film. He concluded that the application and use of Se75 for industrial radiography is applicable for steel thicknesses over (5mm). Also he found that the relative contrast of Se75 is improved compared to Ir192. His results show that the typical welding flaws can be detected using Se 75 <sup>[46]</sup>.

In 2010 Mahrok et.al. present a study on radiography and found that when the radiographed sample is too thin, it is necessary to estimate the effect of the reradiated fluorescent radiation as this was found to contribute significantly to the total transmitted intensity and hence to the contrast <sup>[47]</sup>.

### **1.11 Aim of the Work**

The aim of this project is to study in depth the effective variables that play roles in detection and examination of fabricated welded joints and castings by x-ray radiography.

These variables are geometric image unsharpness, optical density, sensitivity of film and the correlation between the high voltage and contrast.

Particularly the capabilities and limitations of this technique in defecting the type, size, depth and shape of the imperfections are also studied. Also the identification of defects and abnormalities likely to be encountered during the manufacturing process or afterwards may be detected by x-rays.

**Chapter Two**  
**Experimental Part**

## Chapter Two

### Experimental Part

#### 2.1 Introduction

This chapter includes preparation of samples to be examined by x-ray radiography technique where the industrial defects in internal structure of the object in the welded sample or casting is revealed in the x-ray film. Also description of the instruments is included.

#### 2.2 Samples Preparations

Three types of samples were prepared: namely: steel plates, steel welded and casting of aluminum alloy.

##### 2.2.1 Steel Plates

X-ray interacts with any substance that it passes through. This interaction enables different parts of substance to be inspected through the differential attenuation of x-ray. During the passage of x-ray through the substance, their intensities are reduced exponentially. Many factors affecting the reduction in x-ray as it passes through the substances. The mathematical formula expressing this behavior is equation (1.4). The incident and transmitted intensities are proportional to the exposure. Accordingly by using different thicknesses of steel plates, a different value of the ratio ( $I/I_0$ ) can be obtained. These are (15) plates of ( $80 \times 55 \times 4 \text{ mm}^3$ ) in dimension and (2) plates of ( $55 \times 45 \times 1 \text{ mm}^3$ ) in dimension from the same weld metal samples. These plates were arranged as steps with gradual increase in thickness from (2-20 mm). Fig. (2.1) illustrates these arrangements of the samples.



**Fig. (2.1) A photograph illustrates steel plates**

### **2.2.2 Casting Sample**

In order to calculate the size and depth of defects and voids in castings which may occur during production process, an aluminum alloy block was prepared that incorporates two different radii steel spheres. The aluminum alloy liquid was obtained by heating aluminum alloy pieces in a furnace up to the aluminum melting point for (30) minute. Then liquid aluminum alloy was poured in a rectangular mould consist of natural sand has dimension of  $(162 \times 102 \times 61 \text{ mm}^3)$ . Two steel spheres of (28.4 mm) and (18.9 mm) in diameter were prepared as in fig. (2.2). They were embedded inside the mold during pouring the aluminum alloy liquid into the mould. Fig. (2.3) illustrates the casting of aluminum alloy including the steel spheres.





**Fig. (2.2) A photograph illustrates steel spheres**



**Fig. (2.3) A photograph illustrates casting sample of aluminum alloy**

### 2.2.3 Welded Sample

Welded carbon-steel alloy by E7018 wire was used for the evaluation of weld defects that may be occurred in the welding process. Welded sample was steel plates of dimension (200×200×5 mm<sup>3</sup>). The plate edges were processed (tapered) before welding in a butt weld design. The later may take various geometrical forms as (V) or (K) or (X) shape <sup>[7]</sup> (V) shape was used in our investigation according to the requirement. The two plates after the geometrical treatment were adequately cleaned, by a suitable known methods then using arc welding from the side of the prepared edges as illustrated in fig. (2.4).



**Fig. (2.4) A photograph illustrates steel welded sample**

## 2.3 Nondestructive Testing

X-ray radiography which is a nondestructive testing method was used for welding and casting evaluation. This method was performed by placing x-ray film inside light tight holder close to weld region or casting, and irradiating it from the other side. The x-ray tube lens must be aligned to the area to be tested. According to the inverse square law, the distance between the x-ray tube and the object must be determined carefully because this distance is affected by the density, thickness and allowable tube voltages. The variation in the distance between the x-ray tube and object must not exceed certain range where the unsharpness is not allowable.

### 2.3.1 X-ray System

The x-ray equipment used is (RADIOFLEX) and it is Japan made for radiography. Fig. (2.5) illustrates this x-ray system. The main characteristics of this system are as follows:

Tube voltage: variable up to 250 kV

Tube current: variable up to 5 mA

Anode material: Tungsten (W)

Focal Spot Size (F.S.S): 1.5 mm

Exposure time: variable up to 60 minute



**Fig. (2.5) A photograph illustrates the x-ray system**

### **2.3.2 X-ray Film**

X-ray film type (AA400-KODAK) of USA product covered with (0.1mm) lead screen was used in this investigation. This type of x-ray film is suitable for both automatic and manual processing. Exposed x-ray films were processed manually in a dark room according to ASTM-E94-77<sup>[29]</sup> as follows:

- 1-The first step is the dilute process where each of the developer and fixer are diluted with distilled water by the ratio (1:4).
- 2- The second step is immersing the x-ray film in (KODAK) developer for (2) minutes at a temperature of 25°C. Then the film was washed in distilled water.
- 3- The third step is immersing the film in (KODAK) fixer for one minute at 25°C. The film was then washed in fluid water.
- 4- The final step is to dry the film by suspending it in air.

### 2.3.3 Optical X-ray Film Density

The optical density of x-ray film defined as a measure of the degree of blackening of x-ray film , is measured directly by using a transmission densitometer (Grandville, Michigan) of USA product. Fig. (2.6) shows the transmission densitometer used in this work. The x-ray film is placed directly between the light source and the sensitive photodiode of the densitometer to measure the transmission of light. Area of x-ray film with high degree of blackening transmits less visible light as compared to other areas of low degree of blackening. The densitometer is, therefore, programmed to give large digital reading for high degree of blackening and vice versa.



**Fig. (2.6) A photograph illustrates a transmission densitometer (Grandvill,Michigan)used in this work**

### 2.3.4 Geometric Image Unsharpness

Geometric image unsharpness of samples can be calculated according to equation (1.5). Since most radiation sources are too large to be approximated by a point, the used x-ray tube has focal spot size (F) of (1.5 mm) in diameter. From these calculations one can find the best focal to object distance (L) when  $(U_g)$  was proposed from (ASME-section 5. 1985) and it was found equal to (0.5 mm) <sup>[48]</sup>.

### 2.3.5 Characteristic Curves of X-ray Film

The characteristic curves for (KODAK) x-ray film are produced as follows.

a- Steel plates were placed close to the film in the path of x-ray beam and were arranged in steps with increasing thickness. These plates were radiographed three times with an exposure time of (80) second for the following operating condition.

(120) kV: 5mA

(140) kV: 5mA

(160) kV: 5mA

Focal- Object Distance (F.O.D): 700mm

b- Since the exposure factor is directly proportional to  $(I/I_0)$ , hence a measurement of  $(I/I_0)$  was obtained according to equation (1.2) and by using data of  $(\mu / \rho)$  at different energies for all the elements present in our sample<sup>[49]</sup>, we obtained an indication for the exposure (E).

c- The optical density (D) of the x-ray film was measured and plotted against logarithm of (E) which was calculated according to equation (1.6).

d-The calculated film gradient ( $\gamma$ ) was achieved according to equation (1.9). From these measurement and calculations the most

suitable x-ray tube voltage was determined for the samples to be radiographed.

### 2.3.6 Sensitivity Tests for Radiography of Welded Sample

Penetrameter (DIN 62 FE) is commonly used as image quality indicator (IQI). Fig. (2.7) shows these indicators which are used in this work. Every indicator consists of seven wires of typical metal ranging in diameter from (0.250 mm) to (1.00 mm). The percentage radiographic sensitivity was calculated according to equation (1.10). Wire penetrameter is placed close to the surface of the specimen from side of the x-ray source. The thinnest detectable wire on the radiographs is taken as a measure of the radiographic sensitivity.



**Fig. (2.7) A photograph illustrates wire type penetrameter**

### 2.3.7 Measurement of Film Density

#### a- Steel Plates Samples

Optical film densities for different thicknesses of steel plates are measured by using a transmission densitometer as mentioned in section (2.3.3) at the following condition.

Tube Voltage: (120, 140, 160) kV.

Exposure Time: 80 second.

Focal- Object Distance (F.O.D): 700 mm.

Thickness ranging from (2-20 mm)

And the results are tabulated in table (3.2).

#### b- Welded Sample

Optical film densities at different voltages for the welded sample of thickness (5) mm are measured by using the same condition mentioned above. And the results are tabulated in table (3.3).

#### c- Casting Sample

Optical film densities for radiographic casting image are taken at the following condition:

Tube voltage: 70 kV.

Focal- Object Distance (F.O.D): 70 mm.

Exposure Time: 1 second.

Thickness of casting sample: (61mm)

And the results are tabulated in table (3.4). X-ray films are processed as mentioned in section (2.3.2).



## **2.4 Identification of Foreign Materials in Casting by Using X-ray Radiography**

This was performed by taking two radiographs from two opposite sides of the casting mentioned in section (2.2.2) and illustrated in fig. (2.3). The first radiograph was taken from the right side (R) of the casting, and the second radiograph was taken from the left side (L) of the casting. The Focal Object Distance (F.O.D) was fixed at (700 mm). The above procedure was repeated at Focal Object Distance (F.O.D) equals (350 mm). Then the depth of the steel spheres (Y) and their actual radii (R) could be calculated according to the equations (1.12) and (1.13). The operating conditions for the x-ray system were as follows:

Tube Voltage: 70 kV.

Exposure Time: 1sec.

Tube Current: 5 mA.

**Chapter Three**  
**Results and Discussions**

## Chapter Three

### Results and Discussions

#### 3.1 Introduction

This chapter covers the results obtained after testing and analyzing films. These results include the optimum condition of x-ray energy and geometry used to detect and identify the abnormalities either in casting or welding processes.

#### 3.2 Geometric Image Unsharpness Result

(F.O.D) was taken as (700 mm) for the thicknesses in the range (X=5 – 61 mm). (F.O.D) was taken as (350 mm) for thickness (61 mm). The geometric image unsharpness ( $U_g$ ) values were calculated according to the equation (1.5) and compared with allowable ( $U_g$ ) values as shown in table (3.1). The calculated ( $U_g$ ) values are within the allowable limits of ( $U_g$ ) and in fact much lower than it.

From these calculations one can see that the unsharpness ( $U_g$ ) was measured for (F.O.D) equals (350 mm) and (700 mm) and for thickness (5 mm) and (61 mm) respectively. The above values of (F.O.D) and thickness were suitable to result in minimum values of ( $U_g$ ) and this means that no loss in the quality and definition is to be expected

**Table (3.1) Calculated ( $U_g$ ) values compared with allowable limits <sup>[48]</sup>**

<b>Sample</b>	<b>Thickness (mm)</b>	<b>Focal Object Distance (F.O.D)(mm)</b>	<b>Calculated (<math>U_g</math>) (mm)</b>	<b>Allowable Limits of (<math>U_g</math>) (mm)</b>
<b>Welding Sample</b>	5	700	0.01	0.5
<b>Casting Sample</b>	61	700	0.13	0.5
<b>Casting Sample</b>	61	350	0.26	0.5

### 3.3 Optical Density Measurements and Calculations

Optical densities were measured according to condition mentioned in section (2.3.7). The manual processing of the film and any possible contamination may influence the optical density measurement, and this will produce a deviation in the measured density and may increase the error. Therefore, the instruments concerning the chemical processing of the x-ray film should be followed precisely. The densitometer used in this study was first calibrated against standard absorbers. Then the instrument was used to measure the optical densities of the x-ray films obtained in this study after the subtraction of the background density. Table (3.2) shows estimated optical film density for steel plates, While table (3.3) shows estimated optical film density for welded sample. The radiographic contrast was calculated according to the equation (1.8). Table (3.4) shows the estimated optical film density for casting sample.

**Table (3.2) Estimated optical film density for steel plates**

<b>High voltage of x-ray tube (kV)</b>	<b>Steel plates thickness (mm)</b>	<b>Optical film density(D)</b>
120	2	2.86
	4	1.40
	8	0.55
	12	0.35
	16	0.30
	20	0.29
140	2	---
	4	2.92
	8	1.39
	12	0.84
	16	0.59
	20	0.49
160	2	---
	4	3.02
	8	2.19
	12	1.26
	16	0.88
	20	0.68

**Table (3.3) Estimated optical film densities for welded sample and their radiographic contrast**

High voltage of x-ray tube (kV)	Welded sample thickness (mm)	Optical film density (D)		Contrast $C=D_1-D_2$
		D <sub>2</sub>	D <sub>1</sub>	
120	5	0.92	1.22	0.30
140	5	2.54	2.93	0.39
160	5	----	----	----

**Table (3.4) Estimated optical film density for casting sample**

High voltage of x-ray tube (kV)	Diameter of steel spheres shadow (mm)	Optical film density (D) measured								
		At the center	At X-direction				At Y-direction			
70	30	0.34	0.43	0.39	0.41	0.43	0.44	0.4	0.4	0.42
	20	0.43	0.47	----	----	0.46	0.46	----	----	0.45

### 3.4 Defect Interpretation for Welded Sample

Three types of defects were noticed, namely incomplete root penetration, porosity and undercut. The observed defects are in agreement in their description and radiographic appearance with the (AS4749) <sup>[50]</sup>. Typical picture of the radiographs for these defects are shown in fig. (3.1). The radiographic images taken at 120kV and 140kV

show these defects clearly, while the radiograph taken at 160kV does not show these defects because the voltage was too high which made the majority of the photons to penetrate the sample with little differential attenuation. This means that there is suitable tube voltage to radiograph a particular metallic sample of known thickness and density.

In fact, the intensity of x-ray should be homogeneous before interacting with the radiographed object. However, after emerging from the object the intensity is inhomogeneous due to absorption and scattering in different internal structures of the object. Therefore, the image formed on the radiograph is a shadow related to these different intensities due to different structures and appears on the radiograph as black and bright areas. Table (3.5) summarizes the observed defects in welded sample<sup>[50]</sup>

**Table (3.5) A summary of the observed defects in welded sample**

<b>Imperfection</b>	<b>Description</b>	<b>Radiographic Appearance</b>
Incomplete root penetration	Failure of the weld metal to extend into the root area of a joint	Dark intermitted bond with mostly straight edges
Porosity	A group of gas pores confined to a small area of a weld	As a cluster of small dark round indication
Undercut	An irregular groove at the top edge (toe) of a weld	As a dark irregular band along the top edge (toe) of the weld metal

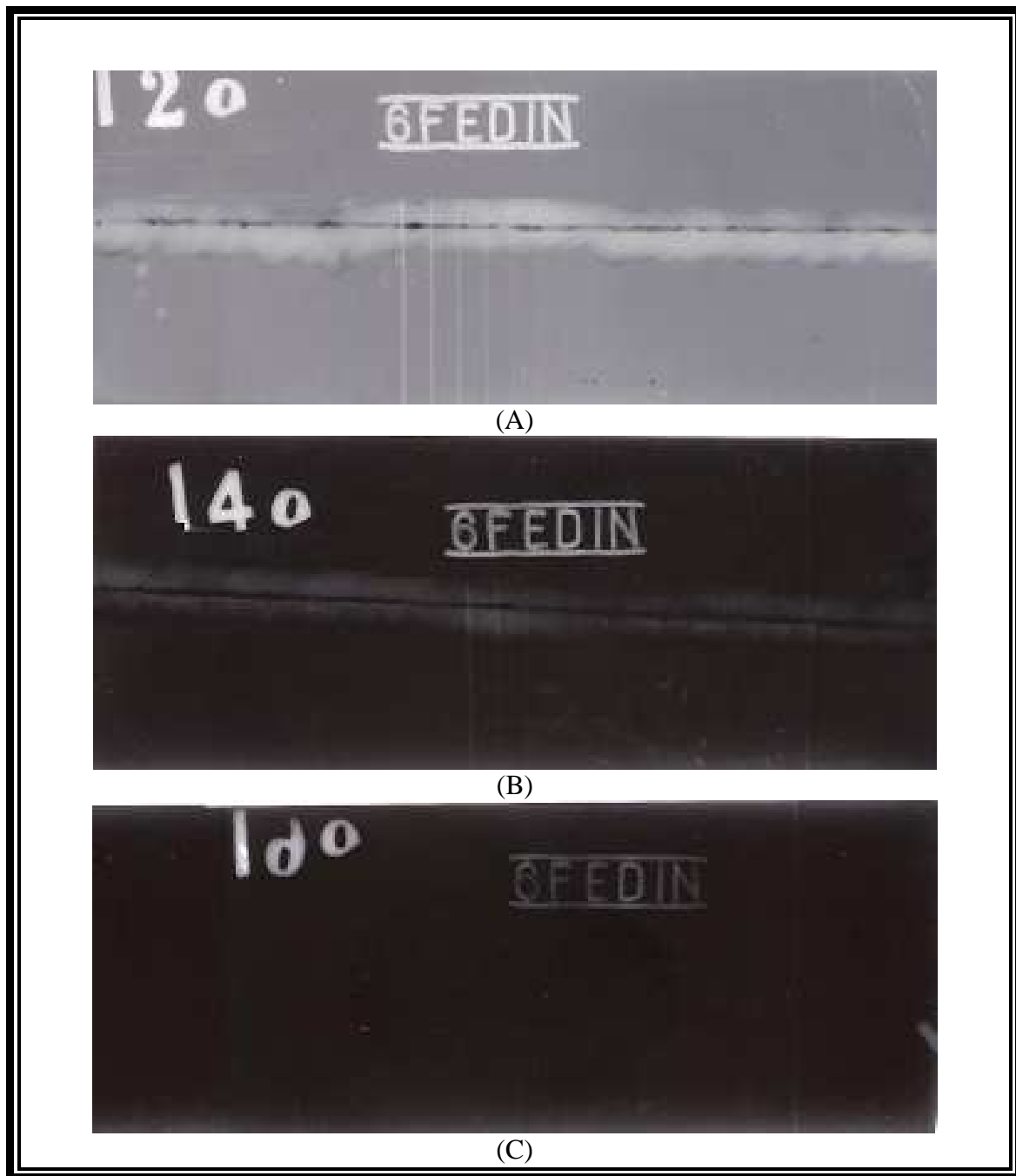


**Fig. (3.1) Typical radiographs for welded sample at different (kV)**  
A: 120kV    B: 140kV    C: 160kV



### 3.4.1 Sensitivity Determination for Welded Sample

The thinnest wire detected of (0.25 mm) was using (120) kV and (140) kV, as shown in Fig. (3.1) (A) and (B). However, when (160) kV is used, none of the wires are detectable because of the high kV which made the photons to penetrate the sample with small differential attenuation.

The sensitivity was calculated using equation (1.10) and listed in table (3.6). It can be noticed from this table that any defect can be detected if its size is (5%) of the radiographed object or more using (120) kV and (140) kV.

**Table (3.6) The percentage radiographic sensitivity at different tube voltages**

High voltage of x-ray tube (kV)	Thinnest detectable wire (mm)	sensitivity
120	0.25	5%
140	0.25	5%
160	-----	-----

### 3.4.2 Characteristic Curves of X-ray Film

Optical film densities for steel plates at different energies, of x-ray photons are presented in figs. (3.2 to 3.4).

Measured characteristic curves for the x-ray film at different voltages of x-ray tube are presented in figs. (3.5 to 3.7). The operating conditions of the system for all experiments were mentioned in section (2.3.5). Using the logarithm of exposure instead of exposure has an advantage to compress the long exposure scale.

The film gradient ( $\gamma$ ) represents the slope of characteristic curves for optical density belonging to the thickness (4 mm) to (8 mm). Fig. (3.8) represents the relation between film gradient and tube voltage. This curve is used to estimate the x-ray tube voltage. Many researcher were used this estimated curve for different industrial jobs <sup>[44]</sup>. The optimum film

gradient ( $\gamma$ ) was found at tube voltage of (140)kV. The reason for producing the characteristic curves and the film gradients derived from them is to find the suitable voltage for range of thicknesses of a material to be radiographed.

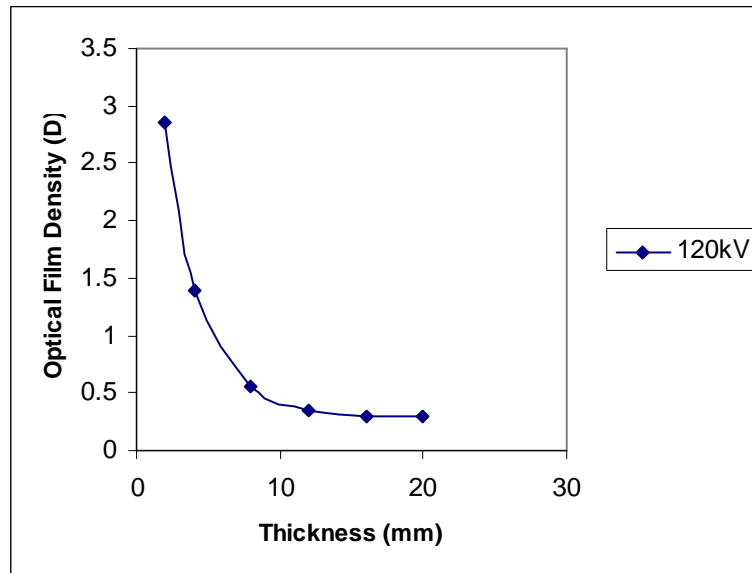


**Fig. (3.2) Optical film density as a function of thickness at exposure time (80) second and tube voltage (120) kV**

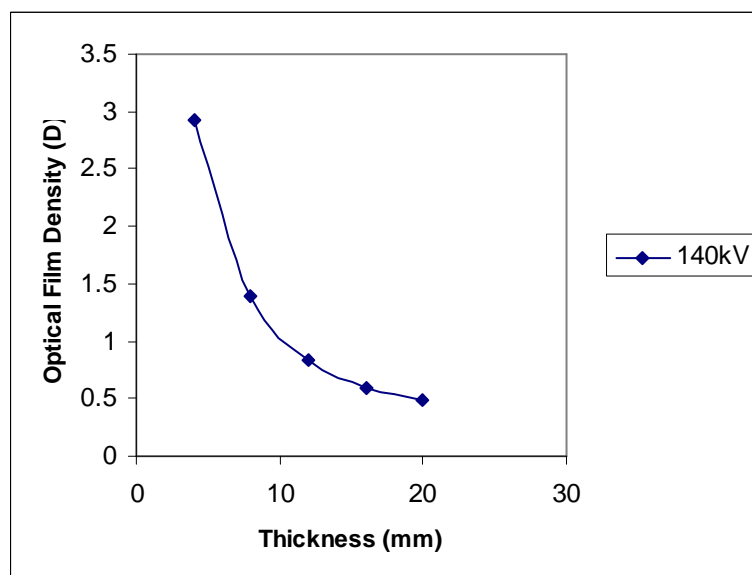


**Fig. (3.3) Optical film density as a function of thickness at exposure time (80) second and tube voltage (140) kV**

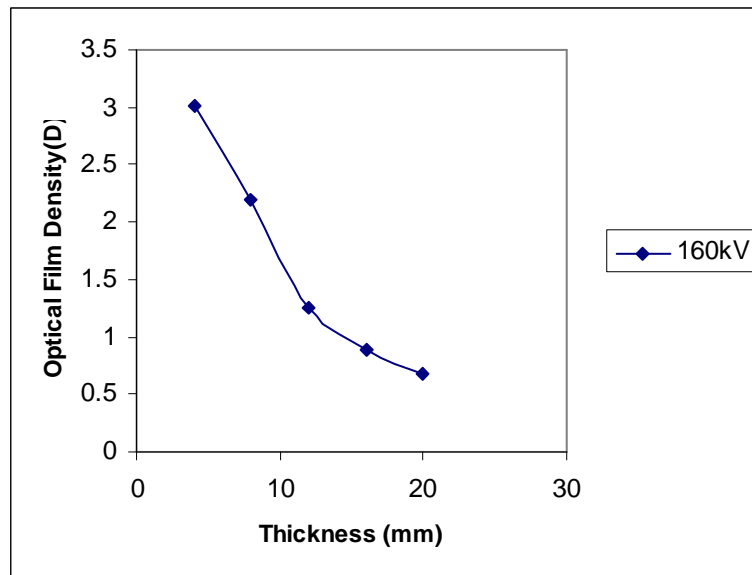


**Fig. (3.4) Optical film density as a function of thickness at exposure time (80) second and tube voltage (160) kV**

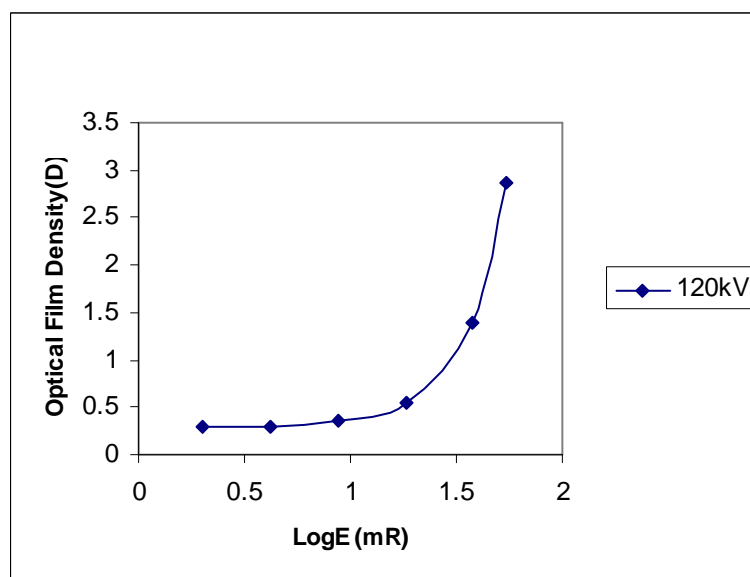


**Fig.(3.5 ) Characteristic curve of x-ray film at tube voltage (120) kV**

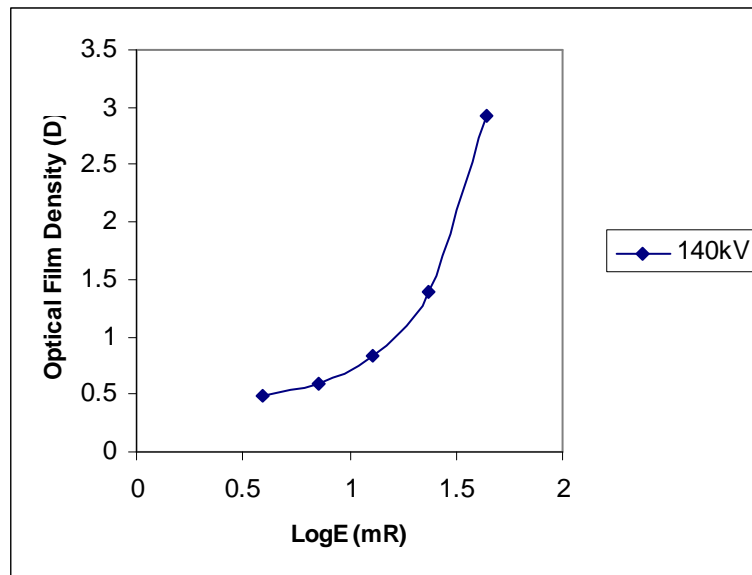


**Fig.(3.6) Characteristic curve of x-ray film at tube voltage (140) kV**

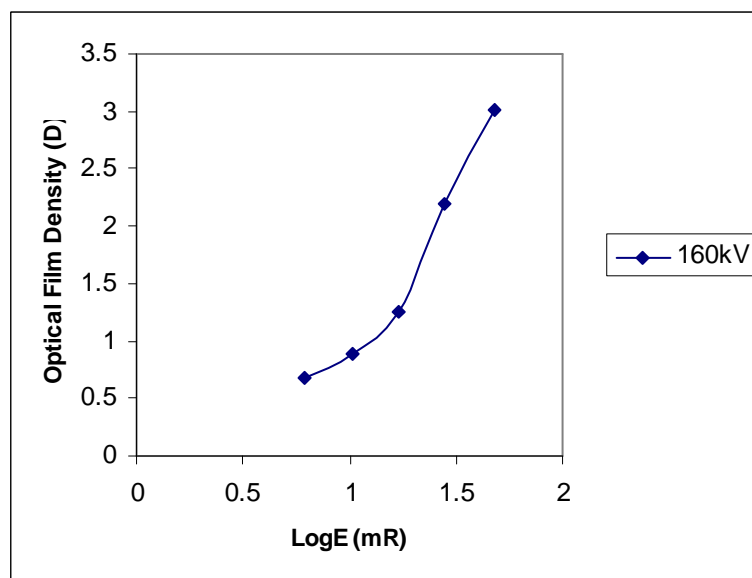


**Fig. (3.7) Characteristic curve of x-ray film at tube voltage (160) kV**

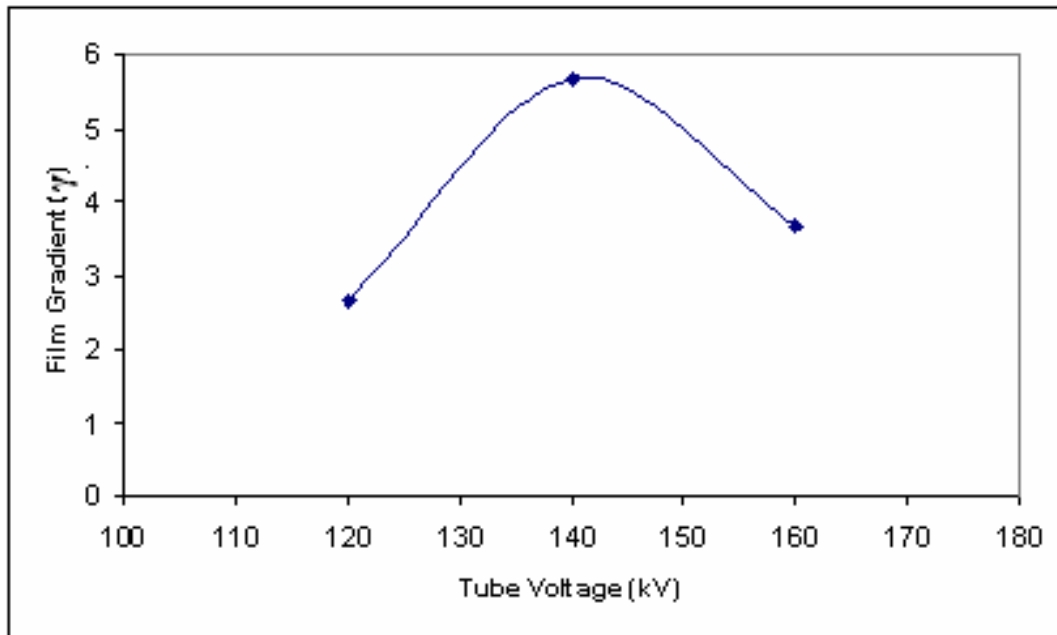


**Fig.(3.8) Film gradient ( $\gamma$ ) at different tube voltages (kV)**

### **3.4.3 Correlation between Characteristic Curves and Welded sample Contrast at Different (kV) and Sensitivity**

Sensitivity for welded sample achieved according to table (3.6) seems to have the same degree of delectability at (120) kV and (140) kV. But from the characteristic curves and their film gradient the results show that the optimum film gradient was found at (140) kV where thickness ranges from (4-8 mm) corresponding to a welded sample thickness (5 mm). This result agrees with a welded sample contrast (0.39) as mentioned in table (3.3) .This contrast is better than those obtained with (120) kV and while the film at (160) kV was found darkening. However, the use of more sensitive penetrameter may improve the detection sensitivity of defect in our welded sample.

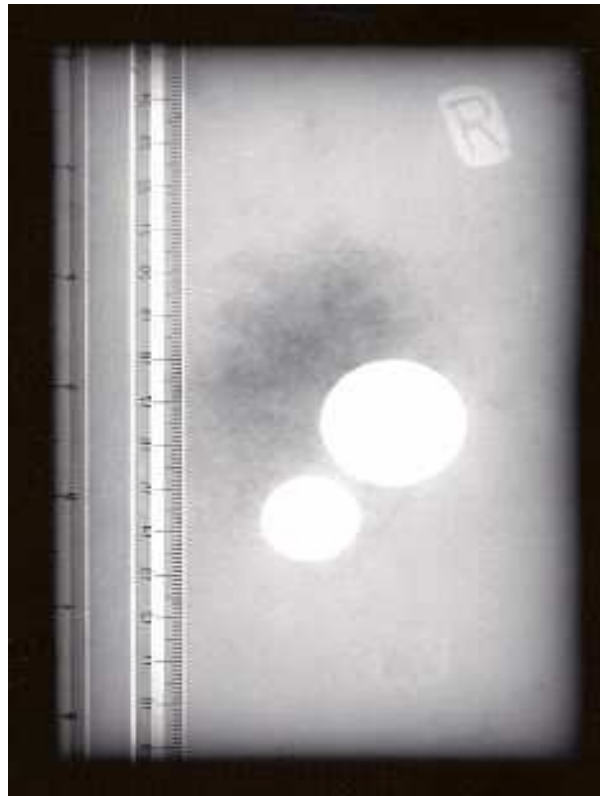
### 3.5 Defects Interpretation for Casting Sample

Two types of defects were noticed namely inclusion (which is represented by two steel spheres embedded in aluminum casting) and segregation. The observed defects are in agreement in their description and radiographic appearance with the (AS3507)<sup>[51]</sup>. Typical radiographs are shown in fig. (3.9) (A and B) for (F.O.D) equal (700 mm). The radiographs shown in fig. (3.10) (A and B) are taken for the same casting sample but for (F.O.D) equal (350 mm). Evaluations of defects were achieved after selecting the best radiographic image at condition mentioned in section (2.4).

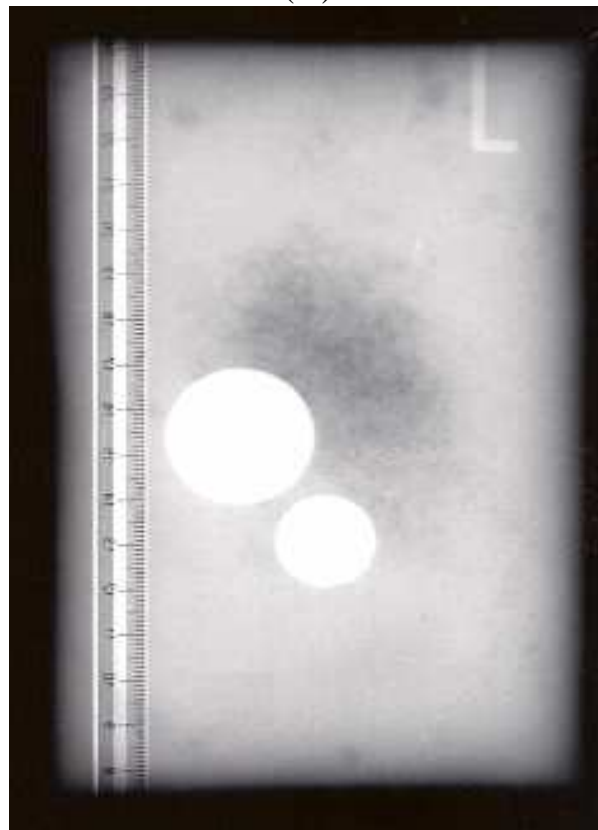
Table (3.7) summarizes the observed defects in casting sample<sup>[51]</sup>.

**Table (3.7) A summary of the observed defects in casting sample**

<b>Imperfection</b>	<b>Description</b>	<b>Radiographic Appearance</b>
Inclusion	Any foreign materials trapped in the metal as it solidifies	As a light or dark shaped image in a radiographs and may be difficult to distinguish from a void
segregation	Particular components of the metal tend to be driven by solidifying metal and segregate at particular area	As a dark area in a radiograph, particularly the central zone



(A)



(B)

**Fig(3.9) Typical radiographs for casting sample at two sides  
A: for right side B: for left side (L=700mm)**



(A)



(B)

**Fig. (3.10) Typical radiographs for casting sample at two sides (L=350mm) A: for right side B: for left side**



### 3.5.1 Identification of Foreign Materials

Radiographic measurement of the shadows of foreign materials and the measurement of the geometrical parameters of the experimental system enabled us to calculate the actual sizes of these materials and their depth inside the casting.

a- For (28.4 mm) in diameter steel sphere embedded in aluminum casting.

The values obtained from the radiographs are: right radius  $R_R=14.5$  mm for side (R) as in fig. (3.9) (A) and left radius  $R_L=15$  mm for side (L) as in fig. (3.9) (B). The (F.O.D) is  $L=700$  mm and the cast thickness  $X=61$  mm. While the values obtained from the radiographs at (F.O.D)  $L=350$  mm are  $R_R= 14.5$  mm as in fig. (3.10) (A) and  $R_L=15.5$  mm as in fig. (3.10) (B).By putting the values above in equations (1.12) and (1.13), the radius (R) and the depth (Y) of the foreign material were found. Table (3.8) represents the calculated values of radius (R) and depth (Y) for steel sphere.

**Table (3.8) Represents the calculated values of radius (R) and depth (Y) for steel sphere**

<b>Focal Object Distance (F.O.D) (mm)</b>	<b>Radius of Steel Sphere (R) (mm) Calculated from Radiographs</b>	<b>Depth of Steel Sphere (Y) (mm) from Side (L) Calculated from Radiographs</b>	<b>Depth of Steel Sphere (mm) from Side (R) Calculated from Radiographs</b>
700	14.1±0.4	18.1±0.4	42.9±0.4
350	13.8±0.4	17.8±0.4	43.2±0.4

b- For (18.9 mm) in diameter steel sphere embedded in aluminum casting.

Let  $R_R$  be the radius of the steel sphere on radiograph (A) when the aluminum casting is radiographed from the right side (A). And  $R_L$  be the radius of the same steel sphere on radiograph (B) when the aluminum casting is radiographed from the left side (B). Then values obtained from the radiographs are  $R_R=9.5$  mm for side (R) fig. (3.9) (A), and  $R_L=10$  mm for side (L) fig. (3.9) (B). The (F.O.D) is  $L=700$  mm and the cast thickness  $X=61$  mm. While the values obtained from the radiographs at (F.O.D)  $L=350$  mm are  $R_R=9.5$  mm as in fig. (3.10) (A) and  $R_L=10.5$  mm as in fig. (3.10) (B). By putting the values above in equation (1.12) and (1.13), the depth (Y) and the radius (R) of the foreign material were found. Table (3.9) represents the calculated values of radius (R) and depth (Y) for steel sphere.

**Table (3.8) Table (3.8) represents the calculated values of radius (R) and depth (Y) for steel sphere**

<b>Focal Object Distance (F.O.D) (mm)</b>	<b>Radius of Steel Sphere (R) (mm) Calculated from radiographs</b>	<b>Depth of Steel Sphere (Y) (mm) from Side (L) Calculated from radiographs</b>	<b>Depth of Steel Sphere (mm) from Side (R) Calculated from radiographs</b>
700	$9.3 \pm 0.4$	$11.7 \pm 0.4$	$49.3 \pm 0.4$
350	$9.2 \pm 0.4$	$11.4 \pm 0.4$	$49.6 \pm 0.4$

The errors associated with (R) and (Y) in table (3.8) and table (3.9) are attributed to the errors related with the measurement of ( $R_L$ ) and ( $R_R$ ). The error related with ( $R_L$ ) and ( $R_R$ ) are estimated to be equals to (0.5 mm).

By substituting the errors above in the suitable equations taken from (Squires), the errors associated with (R) and (Y) in tables (3.8) and (3.9) were obtained <sup>[52]</sup>.

From tables (3.8) and (3.9), one can notice that a good agreement is obtained related with other researcher. (Mahrok and Azeez)<sup>[37]</sup> used a solid clay sphere in their investigation and they obtained similar results when calculated each of depth and radius. This means that the equations for the radius and the depth are valid for large variation in geometrical parameters and when the density of the introduced material in casting is higher or lower than the surrounding medium. The range of (F.O.D) tested in this investigation is rather limited, but there is no reason why these equations should not be applied for other (F.O.D) values commonly used in radiography. The error associated with the measured values of the radii and depths of the spheres is also small.

c- In order to verify that the shadow on the radiograph belongs to a sphere and not a disc, we measured the optical density on the shadow of the steel spheres on the radiograph along x- and y- direction as mentioned in section (3.3) table (3.4). The results of the measurement are shown in figs. (3.11) and (3.12).

The figures show that the optical film density increases gradually from the center of the shadow towards the edges along x- and y- direction. This variation in optical density of the shadow is interpreted as being related to a sphere. However, if there is no variation in optical density between the

edges of the shadow and the center (i.e. flat line); therefore the shadow on the radiograph belongs to a disc and not a sphere.

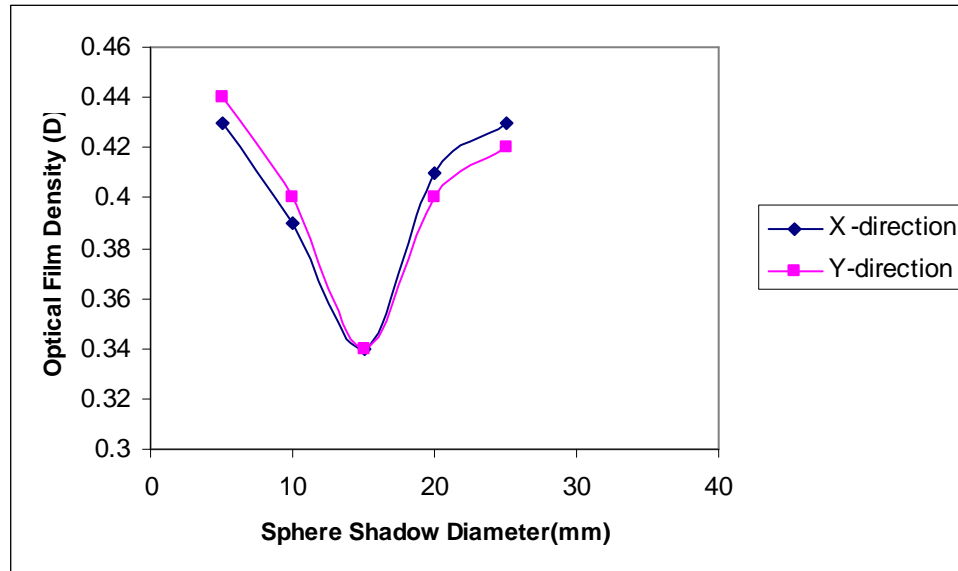


**Fig.(3.11) Optical density variation of (30mm) in diameter of the shadow of a sphere on a radiograph**

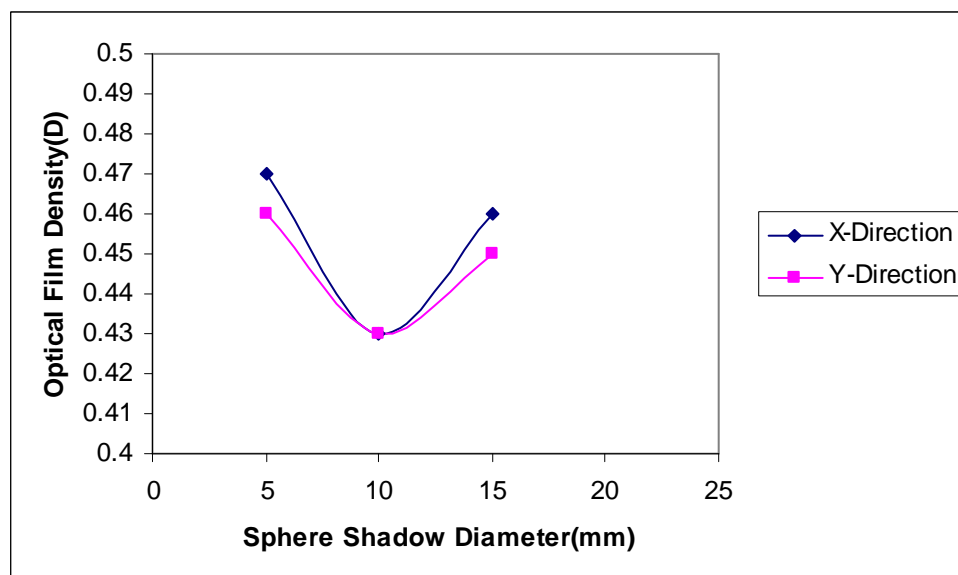


**Fig. (3.12) Optical density variation of (20mm) in diameter of the shadow of a sphere on a radiograph**

## **Chapter Four**

### **Conclusions and Future Work**

## **Chapter Four**

### **Conclusions and Future Work**

#### **4.1 Conclusions**

The main points in this article are.

1- In order to obtain a quality image the operating conditions such as tube voltage (140) kV and focal object distance (700 mm) for thickness of (5 mm) was determined for welded sample inspection.

2- The ultimate goal in radiography is high image sensitivity. This goal was achieved at (120) kV and (140) kV where was found the sensitivity (5%).

3- The formation of the image on the x-ray film depends on film type (medium), exposure time (80) second and the distance between the object and x-ray film (700 mm).

4-X-ray radiography technique can be used as a method for identification and quantification of the type, size and depth of defects in welded joints or castings. Also, the actual shape of the defects can be realized.

5- The two equations derived earlier to find the size and depths of defects are valid whether these defects are higher or lower in density than the surrounding medium. And there is no reason why these equations should not be applied for other (F.O.D) values used in radiography.

## **4.2 Future Work**

1-Identification of defects and abnormalities in welded joints and casting through magnifying these defects by keeping the x-ray film at different distances from the radiographed object rather than putting it in contact with the radiographed object may be tried.

2-Analysis of the radiograph by the aids of computer software to obtain more information from the radiograph may also be tried.

3-Panoramic system of x-ray can be used with aids of motor to detect the imperfection more quickly.

4-Sensitive detector joined with a computer may be used to reduce both of time and cost.

## **References:**

1-Barry Hull., "**Nondestructive Testing**" Macmillan Education, London, 1988.

2- Sagamore A.,"**Nondestructive Evaluation of Materials**", Plenum, New York, 1979.

3- Baldev Raj., Subramanian. C. V., and Jayakumar. T.,"**Nondestructive Testing of Welds**", Narosa Publishing House, New Delhi, 2000.

4-Baldev Raj.,and Jaya Kumar T., "**Review of NDT Techniques for Structural Integrity**", Sadhana, Indian Academy Proc. In Engineering Sciences, Vol. 20, pp. 5-38, 1995.

5-Sharpe R. S.,"**Quality Technology**", 4<sup>th</sup> edition, NDT Center Harwell Publishing, 1984.

6-Lancaster J. F.,"**The Metallurgy of Welding, Brazing and Solidering**", George Allen and Unwin, London, 1971.

7-Eurocode3:"**Design of Steel Structure**"ENV, 1993-1-1: General Rules and Rules for Building, CEN, 1992.

8- Khanna M.,and LAL O. P., "**A Text Book of Foundry Technology**" 2<sup>nd</sup> edition Published by j-c Kopour, 1979



9-Carlson K. D., "**Modeling of Casting, Welding and Advanced Solidification Processes**", ed, DM. Stefanescu. warrendale, PA: TMS, pp. 295-302, 2003.

10-Sigl K. M., "**Fatigue of Cast Steel in The Presence of Porosity**", International Journal of Cast Metals Research, Vol. 3, pp. 130-140, 2004.

11- Lai N. W., Griffiths W. D., and Campbell J., "**Modeling of Casting, Welding and Advanced Solidification Processes**", ed. D. M.Stefanescu. Warrendale, PA, TMS, pp. 415-422, 2003.

12- Campbell J., and Clyne T. W., "**Study of Hot Tearing in Aluminum Alloys**", Cast Metals, Vol. 13, pp. 453-460, 1991.

13- Kluska S. et.al., "**Diagnostics of Crack Formation in Castings using the Logic of Plausible Reasoning**", International Scientific Journal, V. 28, No. 8, pp. 479-482, 2007.

14-Siekanski K., and Borkowski S., "**Analysis of Foundry defects and Preventive Activities for Quality Improvement of Castings**", Metalurgija, Vol. 42, No. 1, pp. 57-59, 2003.

15- Hogarth G. H., "**Techniques of Nondestructive Testing**" Butterworth and Co., 1959.

16- Ditehburn R. J., "**NDT of Welds State of The Art**", NDT and International, Vol. 29, No. 2, p. 111, 1996.

- 17- Achenbach J. D., "**Solid Mechanics Research for Quantities Nondestructive Evaluation**" The kluwer Academic Publishers Group, 1987.
- 18- American Standards of Mechanical Engineering ASME-Section.5, 1983, USA.
- 19- American Society for Metals, "**Metals Hand Book**", Vol. 11, 1986, USA.
- 20- Fontana M. G., "**Corrosion Engineering Reference Book**", Mcgraw Hill, New York, pp. 41-42, 1986.
- 21- Halmshaw R., "**Nondestructive Testing**" 2<sup>nd</sup> edition, published by Edward Arnold, 1991.
- 22- Sharpe R. S., "**Research Techniques in Nondestructive Testing**" NDT center Harwell, Vol. 3, 1981.
- 23- Adams R. D., "**Ultrasonic Inspection of Ceramic Bearings**" Journal of Advanced Materials and processes, Vol. 150, p. 27, 1996.
- 24- ASTM- E.587-76. "Standard Method for Determination Relative Image Quality Response of Industrial Radiographic Film", p.572, USA.
- 25- Segal Y., "**Limitations in Gap Width Measurements by X-ray Radiography**" Journal of NDT International, Vol. 21, No. 1, pp. 11-16, 1988.

26- Gaalr Weymueller., "**Know your Welding NDT-radiographic Testing**" Journal of Welding Design and Fabrication, March, 1983.

27-Ghoshal S., "**Modren physics**", Published Chand, Delhi, 2004.

28- Huggins B. E., "**Radiography with Low Energy Radiation**" The British Journal of NDT, Vol. 23, NO. 3, p. 119, 1981.

29-ASTM Designation: E.94-77, "Standard Recommended Practice for Radiographic Testing", USA.

30-Deny Y. S., "**Study of Geometric Imaging in Radiography**" NDT International, Vol.22, No.6, pp.353-358, 1988.

31-Meredith W. J., and Massey J. B., "**Fundamental Physics of Radiology**" 3<sup>rd</sup> ed, Wright, Bristol: John Wright and Sons LTD, Manchester, 1977.

32-Nielsen Jens Als., and Morrow Des Mc., "**Elements of Modern X-ray Physics**", John Wily and Sons LTD, New York, 2001.

33- Germany Stander Designation DIN62CU, 1980.

34- British Standards Institution, "**Specification for Image Quality Indicators for Industrial Radiography**", BS3971, 1980.

35- ASTM Designation: E 142-77, "Standard Method for Controlling Quality of Radiographic Testing ", USA.

36- Mahrok F. M., and Azeez B. A., "**Method of Identification of Foreign Materials Embedded in Metals by X-ray**", Raf. Jour. Sci, Vol. 12, No. 3, pp. 108-112, 2001.

37-Charles J. H., "**Hand Book of Nondestructive Testing**", MsGraw-Hill, Madrid, 2003.

38- Kriesz H., "**Radiographic NDT- a review**" The Independent Journal of Non-destructive Testing. Vol. 12, No. 6, 1979.

39- American Welding Society, "**Brazing Manual**", published Reinhol, 1960.

40- Stewart P. A. E., "**Advances in Radiology and Fluoroscopy**" British Journal of NDT, Vol. 42, pp. 27-32, 1982.

41- Adams. R. D., "**Review of Defect Types and Nondestructive Testing Techniques, for composites and Bonded Joints** " Journal of NDT international, Vol. 21, No. 4, pp. 208-228, 1988.

42- Bushlin Y., and Notea A., "**Sizing of slits by Digital Radiography**", NDT International, Vol. 21, No. 6, pp. 397-402, 1988.

43- Deutsch M., Notea A., and Pal D., "**Invention of Abel's Integral Equation and its Application to NDT by X-ray Radiography**", NDT International, Vol. 23, No. 1, pp. 32-38, 1990.

- 44- Jedran A. K., "**Non-destructive Evaluation of Ceramic to Metal Joining**" M.Sc. thesis, Department of Physics, College of Science, University of Baghdad, 2001.
- 45- Ayad M. S., "**Panoramic X-ray Mode for Testing Weld Quality of Natural Gas Pipeline from Khoms City to Tripoli**", NDT International, Vol. 8, No. 8, pp. 1-9, 2003.
- 46- Hayward P., "**Radiography of Welds using Selenium 75, IR192 and x-rays**", Asia-pacific conference on NDT, Auckland , New Zealand, 5<sup>th</sup> – 10<sup>th</sup>, Nov, 2006.
- 47- Mahrok M. F., Jabbar T. A., and Abdulfattah A. A., "**Radiation Contrast Improvement by Suitable Choice of X-ray Radiation Spectrum**", Accepted in Iraqi Journal of Science, 2010.
- 48- American Standards of Mechanical Engineering ASME-section 5, 1983.USA
- 49-Storm G., and Israel H. I., "**Photon Cross-Section from 1keV to 100 MeV for Elements Z=1 to Z=100**", Nuclear Data Tables AZ, pp. 565-681, 1970.
- 50-AS4749., "**Non-destructive Testing Terminology of Abbreviations for Fusion Weld Imperfections as Revealed by Radiography**", 2001.
- 51-AS3507., "**Non-destructive Testing-Radiography of Steel Castings and Classification of Quality**", 2001.

52- Squires., " **Practical Physics**", Mc Graw Hill, publishing company,  
1968.

## في ذكرى الشهيد الدكتور مازن فضيل مبروك

أستاذي وقدوتي المغفور له الدكتور مازن فضيل اذكرك اليوم  
والذكرى تطل عزيزة خالية كما أطلت طيلة اياما مضت لقد علمتنا أن  
الستائر تستطيع أن تعجب الشمس ولكننا أبداً لن تعجب الأفكار لقد  
علمتنا أن الإنسان لا يكون بمقدار السنين التي يعيشها بل بمقدار  
العطاء الذي يعطيه لأمله ووطنه وأخيراً لا أملك إلا نعمة الدعاء وما  
أروعهما... لحظات أوقف فيها بين يدي الله تعالى مهتملاً أن يجمعنا بك  
في جنات الخلد ..

فرقد

## الخلاصة

يهدف مشروع البحث إلى كشف ودراسة وتقييم العيوب التي تتخلل المصبوبات المعدنية و مفاصل اللحام من خلال تعريضها للأشعة السينية كونها إحدى تقنيات الفحص الأتلافي. تمت دراسة وتحديد أفضل الظروف التشغيلية الكفيلة بأعطاء أوضح وادق صورة شعاعية لشكل وحجم العيب داخل المصبوبة أو المفصل اللحامي.

تم الاعتماد على معادلات رياضية مشتقة مسبقا لاغراض إيجاد حجم وعمق العيوب في المصبوبات المعدنية بأختلاف أنواعها ومفاصل اللحام لاختبار مدى تأثير عوامل الاعتبارات الهندسية على تقنية التصوير الشعاعي.

لقد نوقشت أهمية الفحوصات الأتلافية في الصناعة وبالذات تقنية التصوير الشعاعي بواسطة الأشعة السينية لما لها من ميزات إيجابية عديدة تميزها عن التقنيات الأخرى المستخدمة فمثلا لايمكن كشف أو تحديد بعض العيوب التي تنتج في مفاصل اللحام بأستخدام تقنيات أخرى ولكن عند أستخدام تقنية التصوير الشعاعي بالأشعة السينية مكننا من كشف و تحديد تلك العيوب وبدقة عالية.

تم تحضير نوعين من النماذج الأختبارية لاغراض التصوير الشعاعي أحدها يمثل مصبوبة المنيوم تتخللها كرتين مختلفتي الحجم و معلومتي الأبعاد. تم تصوير نموذج مصبوبة الالمنيوم من جهتين متعاكستين بالأشعة السينية على التوالي لاغراض تحليل ودراسة صورة العيب بدقة أكبر. أما النموذج الثاني والذي يمثل صفيحتين من أفلوآذ تم لحامهما بتقنية القوس الكهربائي وبعدها صور المفصل اللحامي بتقنية الأشعة السينية. تم تحديد عدد من عيوب اللحام في هذا النموذج مثل عدم أكتمال نفاذية مادة اللحام وحزوز عميقة تحت منطقة اللحام وكذلك ظهور كثافة مسامية في منطقة المفصل اللحامي. أن جميع تلك العيوب قد تم تحديدها وكشفها من خلال أستخدام تقنية التصوير الشعاعي.

تم دراسة مختلف الظروف التشغيلية و التحضيرية المؤثرة في كفاءة الكشف للوصول إلى أفضل طرق تحضير و أدق صورة مأخوذة من خلال تحديد العوامل المؤثرة في كفاءة تقنية التصوير الشعاعي. وأخيرا تم اقتراح عدد من مشاريع البحث المستقبلية ذات العلاقة بتحسين اداء كشف وتحديد العيوب الأداخلية للمصبوبات و مفاصل اللحام وتطوير تقنية التصوير الشعاعي بالأشعة السينية في الحقول الصناعية .

صور نموذج اللحام بثلاث فولتيات عالية مختلفة (120 , 140 , 160 ) كيلو فولت على التوالي مع وقت تعرض (80) ثانية . وجدت افضل صورة حيث تكشف العيوب بوضوح إذا كان حجمها (5%) من النموذج المصور عند (120) و (140) كيلو فولت. الى جانب ذلك بينت النتائج الأخرى انه تم العثور على التدرج الامثل للفلم عند (140) كيلو فولت والتباين في الفلم كان أفضل من التصوير عند (120) كيلو فولت وتم الحصول على صورة قائمة بأستخدام (160) كيلو فولت .



أما في مجال مصبوبة ألألمنلوم أثبتت المعادلات المشتقة مسبقا قدرتها كوسيلة لتحديد كل من حجم وعمق العيوب في المصبوبات ومفاصل اللحام .



جمهورية العراق  
وزارة التعليم العالي والبحث العلمي  
جامعة النهرين/ كلية العلوم  
قسم الفيزياء

## دراسة الفجوات المصنعة بهيئة عيوب بواسطة الاشعة السينية لمصبوبة المنيوم ومفاصل لحام الفولاذ

رسالة مقدمة الى  
قسم الفيزياء/كلية العلوم/جامعة النهرين  
كجزء من متطلبات نيل درجة ماجستير في الفيزياء

من قبل  
فرقد رشيد سعيد الزبيدي  
بكالوريوس علوم فيزياء

بإشراف

د. ثامر عبد الجبار جمعة

د. مازن فضيل محروك

شعبان 1431  
آب 2010